Pseudo-Stereo Audio Processor

By
Zachariah Bunce

Advisor
Dr. Vladimir Prodanov

Senior Project
Electrical Engineering Department
California Polytechnic State University
San Luis Obispo
Spring 2019

Table of Contents

List of Tables and Figures

Abstract

Due to both technical and resource limitations, non-professional audio production must often record with a single microphone, creating a mono audio signal. Even some originally multi-channel audio files often combine the separate channels into a single channel to save memory. However, this channel limitation makes any music held within the audio duller during listening. The Pseudo-Stereo Audio Processor remedies this situation, introducing a quadrature phase shift onto a given single-channel audio signal, producing multiple phase shifted output signals. These separate fixed-phase output signals are then recombined to produce a variable phase difference, emulated two-channel version of the input signal, allowing for an easy post-production sound quality enhancement of a single-channel signal that independent or small-scale audio recording studios could utilize. Further, this method of quadrature filtering produces completely decorrelated output signals using a Hilbert Transform, creating unique auditory effects useful in certain aspects of psychoacoustic research much harder to obtain through other means.

Introduction

Of key importance to most audio recordings in the digital age is both the stored quality and digital size. Though an ideal storage medium would maintain the full breadth of recorded quality in every version of a song, oftentimes this quality must decrease to reduce the digital size. For a stereo (two-channel) recording, removing one channel easily accomplishes this data size reduction, halving the data requiring storage. Though this allows for a greater preservation of the full harmonic profile at the same digital size, it eliminates any spatial effects present in the original recording. Furthermore, to even achieve spatial effects within a song in the first place, the original recording environment requires multiple microphones, limiting high quality stereo audio to large recording studios able to purchase multiple high-quality microphones.

However, both a song with erased stereo qualities and one originally lacking in stereo qualities equally benefit from post-recording processing emulating a stereo-like effect. Discussed in [8], the use of an all-pass network can emulate both the depth of traditional stereo audio and create spatial effects unique to pseudo-stereo. As explained in this article, the phase-altering properties of certain all-pass filters contain the key to creating these spatial effects, as on a basic tonal level, a phase shift is simply a time shift proportional to the period. Thus, intuitively, the human ear interprets the phase difference between left and right as the travel time of the sound wave to reach one ear over the other and calculates the source position accordingly. However, this simplistic explanation breaks down when moving beyond single tones. The non-periodic signals that make up most audio recordings are often represented as a stacked continuum of sinusoidal waves at different amplitudes and frequencies, and as the all-pass network introduces a fixed phase shift over all frequencies, the time shift of each component wave changes. This separates pseudo-stereo techniques from common spatial auditory effects such as chorus and produces the unique spatial effects mentioned previously, as the signal variation in time is further varied over frequency.

Building on this idea of phase-separated output channels, many current attempts at producing pseudo-stereo signals outlined in [9] rely on methods such as the physical placement of loudspeakers, digital combinations of IIR all-pass filters to produce comb-like effects, or the partial decorrelation of two copies of a signal through software algorithms. Taking both the method, and the base circuit [7], from single-sideband radio modulation, this project improves upon these partial methods and mathematically utilizes a Hilbert Transform to produce completely decorrelated, orthogonal versions of the input and its inverse. This complete separation enhances the unique effects of pseudo-stereo and provides a more general solution over the highly tuned filters used elsewhere with no leftover correlated components to optimize away.

Though a polyphase filter alone would technically provide all the processing necessary to produce the signals required for a pseudo-stereo audio signal, most users would struggle to operate the device. Thus, the Pseudo-Stereo Audio Processor encompasses a complete system capable of providing its processing abilities to those no more familiar with operating electronics than plugging cables into a USB connector and a 3.5mm audio jack. This expansion of the expected capabilities allows for a much more complex system utilizing both modern high efficiency audio amplification methods [12] and a single-rail low voltage supply. Furthermore, the availability and precision of modern active devices such as op-amps allows for improvements to the largely passive networks originally employed by [5], [6], and [7] through easy buffering and accurate active filters, combating many drawbacks of purely passive networks.

Requirements & Specifications

This section provides a list of and justifications for the specifications laid out during the project planning phase which drove the initial design process.

Table 1: Pseudo-Stereo Audio Processor Requirements and Specifications

Marketing Requirements	Engineering Specifications	Justification
4	The system should operate across a frequency range of 70 Hz to 15 kHz.	Ensures successful operation over the most audible portions of the standard human hearing range. [1]
1, 2, 3, 6	The system should operate from a single-ended voltage supply with a rail voltage of 5V.	Most consumer applications do not have a dual rail supply available, and 5V satisfies the USB standard used by many common consumer power sources.
6	The average power draw from the rail should not exceed 0.5 W.	Ensures low power operation while not over-constraining usage.
5	The outputs should consist of a 0˚, 90˚, 180˚, 270˚, and a two-channel variable degree phase shift of the input signal.	Widens possible uses while not overly constraining the design as most polyphase filters produce all four of the phase-shifted outputs. [2], [3], [5], [6], [7]
3, 4	The variable phase shift output should range from a 0˚ shift to a 180˚ shift within the 70 Hz to 15 kHz range.	Ensures an adequate range of the variable shift output.
3	The variable phase shift output should connect to a common consumer audio connector such as a 3.5mm jack.	Allows for quick testing and usage with widely available devices, such as headphones.
3	A user-accessible control should provide an amplification/attenuation of +20 dB to -80 dB to the magnitude of the variable phase output signal.	Allows for easy external tuning of the audible output volume.
3	A user-accessible control should regulate the variable phase shift amount.	Allows for easy external tuning of the variable output signal.
4	The input should consist of an audio signal in the 70 Hz to 15 kHz range.	Ensures input signal within expected operating range.
4, 5	The total harmonic distortion of any output loaded with 32Ω should not exceed 2% across the frequency range of 70 Hz to 15 kHz under a $1V_{p-p}$ input.	Prevents audible distortions occurring based on standard human hearing detection of nonlinearities under the load conditions of a high-end headphone impedance. [4]
4, 5	The relative phase error of each output compared against the expected quadrature should not exceed ±4˚ across the frequency range of 70 Hz to 15 kHz.	Ensures accurate outputs based on previous research on the behavior of polyphase filters. [2], [4]
1, 2	The physical size should not exceed 7”x5”x2”	Keeps the device on a hand-held scale while not overly limiting physical size.
5	The internal gain of any output signal should not exceed ±10 dB of the input signal across the frequency range of 70 Hz to 15 kHz.	Prevents excessive signal attenuations by the system or output amplitudes exceeding designed operating ranges before the user volume control.
1	The material costs should not exceed $50.	Allows the device to compete with the purchase of a second microphone to achieve stereo audio recording.

Marketing Requirements

1. Low cost
2. Portable
3. Simple to operate
4. Audio frequency range
5. Accurate quadrature outputs
6. USB Powered

Project Planning

This section provides the initial planning stages of the project from a time and cost management perspective. The inclusion of Gantt charts and cost estimate tables provide insight into early planning in the development process.

Time Estimates

Due to the relatively low complexity of the main subsystem, the polyphase filter [7], the time available allows for multiple design iterations, as seen in ***Figure 1*** and ***Figure 2***. Scheduling these iterations using PERT calculations to allot approximately a week to each step of the design process results in four full iterations ending well before the project deadline as seen in ***Table 2***. In addition, the symmetric development breakdown between Winter 2019 quarter and Spring 2019 quarter ensures adequate progress to show in the EE 461 demo.

Table 2: Pseudo-Stereo Audio Processor Deliverables

Delivery Date	Deliverable Description
12/10/2018	EE 460 Final Project Plan Report
2/1/2019	Design Review
3/15/2019	EE 461 demo
3/15/2019	EE 461 report
6/7/2019	EE 462 demo
11/5/2018	ABET Sr. Project Analysis
6/7/2019	Sr. Project Expo Poster
6/7/2019	EE 462 Report

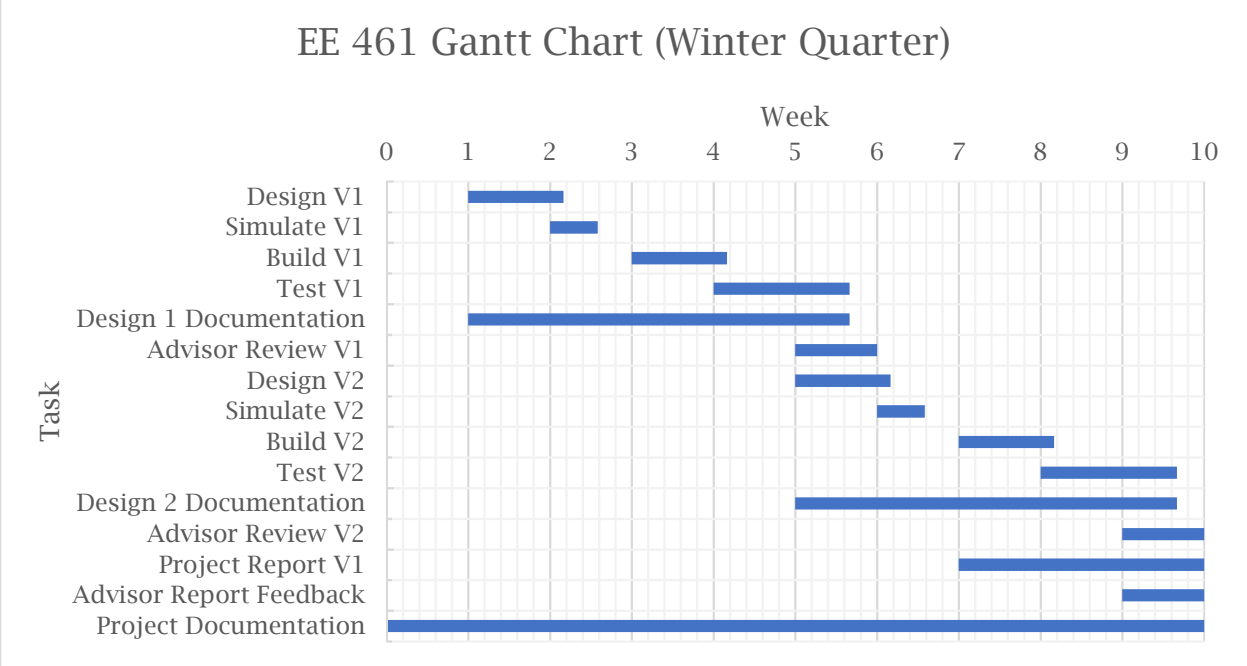

Figure 1: Winter Quarter 2019 Gantt Chart

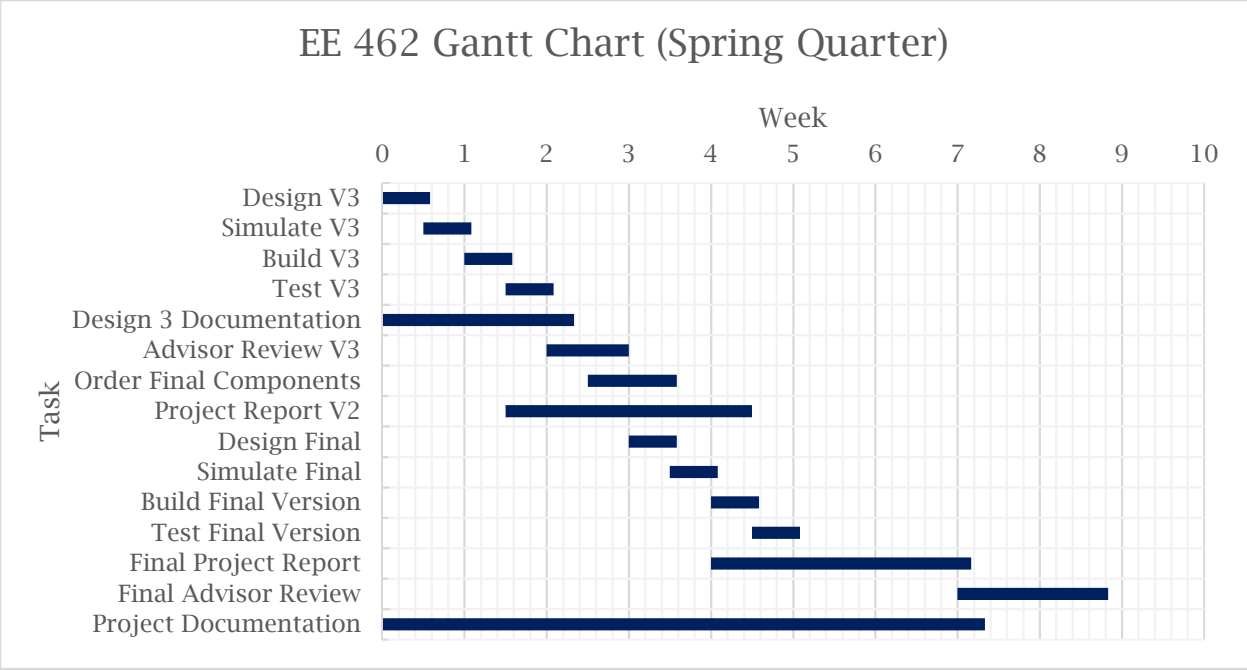

Figure 2: Spring Quarter 2019 Gantt Chart

Cost Estimates

Using the worse-case time value of 180 hours from the average project length of 150 to 180 hours, the labor cost calculation assumes a pay rate of $50 per hour resulting in a total labor cost of $9000 shown in ***Table 3***. Additionally, the material cost estimate shown in ***Table 4*** at $24.72 per design cycle results in a total cost over eight design cycles of $197.60. Though the time estimate in ***Figure 1*** and ***Figure 2*** only accounts for four design cycles, the conservative cost estimation accounts for twice the minimum material necessary. Based on the largely passive component implementation of the polyphase filter seen in [5], [6], and [7], the price per build of $24.72 per cycle further considers a small number of more expensive components to allow for modifications based on [2] and [3]. Rounding out the total cost estimate, the equipment estimates in ***Table 5*** account for any necessary testing and operation costs, resulting in a $1034 estimate. Summing these three main component costs resulted in an overall project cost estimate of $10231.60, as shown in ***Table 3***.

Table 3: Initial Project Cost Estimate

Type	Quantity	Time (Hr)	Cost/Unit ($)	Cost ($)
Labor	1	180	50	9000
Material	8	1	24.72	197.60
Equipment	1	1	1034	1034
Total Project Cost				**$10231.60**

Table 4: Initial Material Cost Estimate

Type	Quantity	Design Cycles	Cost/Unit ($)	Cost ($)
Resistors (1% Tol.)	44	8	0.03	10.56
Capacitors (10% Tol.)	44	8	0.1	35.2
ICs	5	8	2	80
Connectors	8	8	0.5	32
PCB	1	8	5	40
Total Cost per Design				24.72
Total Material Cost				**$197.76**

Table 5: Initial Equipment Cost Estimate

Type	Quantity	Cost/Unit ($)	Cost ($)
Oscilloscope	1	400	400
Power Supply	1	300	300
Multimeter	2	10	20
Function Generator	1	250	250
Oscilloscope Probes	2	7	14
Misc. Connection Wires	10	3	30
2-Channel Earbuds	2	10	20
Total Equipment Cost			**$1034**

Initial Design

Due to the high number of relatively independent analog circuits found while outlining the system from a hardware perspective rather than simply a functional one, the subsequent subsystem breakdown illustrated in ***Figure 3*** lead to a modular design and test approach over the course of the project. As such, the following presentation of the design process flows from one subsystem to another chronologically.

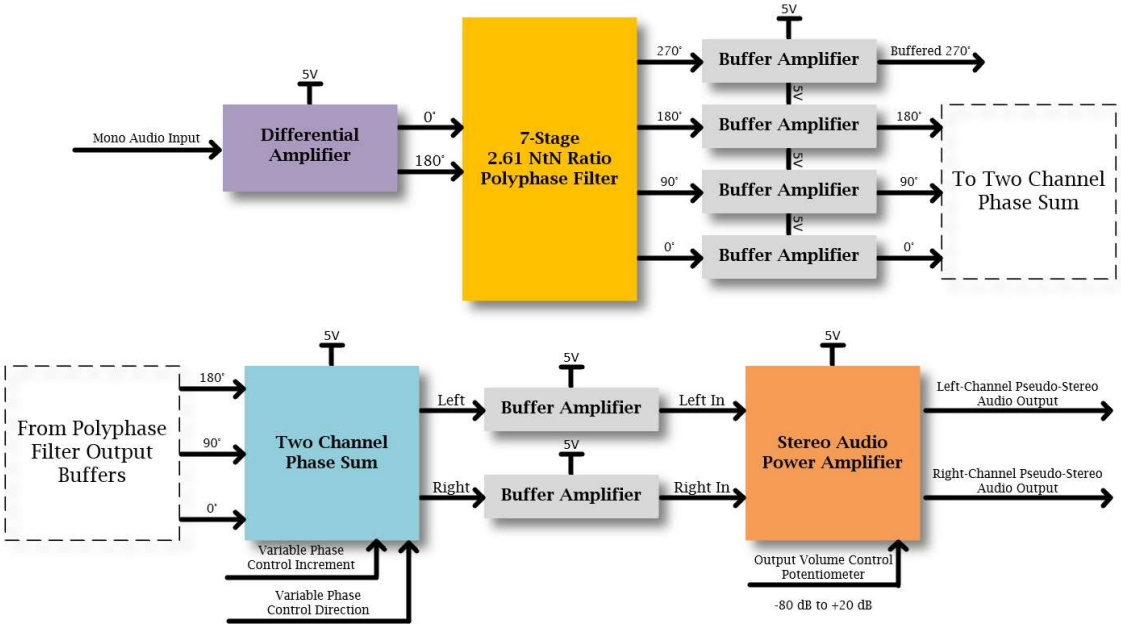

Figure 3: Initial Design Sub-System Decomposition

Polyphase Filter (PPF)

The design began with the component central to the Pseudo-Stereo effect, the Polyphase Filter. Though active topologies such as those presented in [2] and [3] provide a performance increase over the simple passive network of [7], preliminary simulations indicated that a passive filter around five to seven stages met the project specifications with a max attenuation near 7 dB. Deeming the additional performance and corresponding complexity of an active filter unnecessary, the passive topology won out.

Based on the process outlined in [6], the project advisor created an Excel spreadsheet for calculating optimal component values (See **Appendix B** for the final spreadsheet in .csv text format). After modifying the spreadsheet to allow for larger stage counts, the iterative use of this spreadsheet alongside SPICE simulations illuminated key relationships between design parameters. Particularly, the Notch-to-Notch (NtN) ratio and stage number proved most important, as these values controlled the compromise between phase accuracy and passband bandwidth, with a lower Notch-to-Notch ratio indicating higher phase accuracy for a given notch bandwidth and stage count, and a higher stage count increasing the achievable passband bandwidth at each phase accuracy level. As a note, “passband bandwidth” refers to the effective frequency band under which the phase difference is within a given tolerance while in the all-pass input configuration, and “notch bandwidth” refers to the frequency band between the highest notch frequency and lowest notch frequency when in the comb input configuration. See [2] and [3] for more visual examples. Simulations also confirmed that the “Fixed-R” method, under which all stages used the same resistor value while varying the capacitor values, produced the least peak magnitude attenuation. This effectively quantized the allowed Notch-

to-Notch ratios due to the small amount of standard capacitor values, leading to the three Notch-to-Notch values used: 2.154 for ±1˚ of accuracy, 2.612 for ±3˚, and 3.152 for ±5˚.

With this Notch-to-Notch ratio constraint, the design procedure consisted of fixing the Notch-to-Notch ratio and stage count cells in the spreadsheet and iteratively choosing values of lowest notch frequency and per-phase resistance until realizable capacitances produced a simulated design covering the target frequency band. The Notch-to-Notch ratio was then returned to a variable cell, and the notch frequency calculated for the last stage became the highest notch frequency input. Further modifying the spreadsheet to calculate the difference between the capacitance of each stage and the nearest standard value allowed iterative per-stage resistance optimization to minimize this capacitor value variance as a final step.

Following the process described above created a set of four filters, two 5 stage filters and two 7 stage filters each near either the 2.154 or 2.612 Notch-to-Notch ratios. ***Figures 4-7*** contain the simulated frequency response of each filter, while the bottom of the spreadsheet in **Appendix B** contains the component values, upper and lower notch frequencies used, and the simulated passband bandwidth cutoff frequencies for each design. After testing all four filters as shown in **Testing & Construction**, the wide bandwidth and decent phase accuracy of the 7 stage, 2.611 Notch-to-Notch ratio filter caused it to be the filter used as seen in ***Figure 8***.

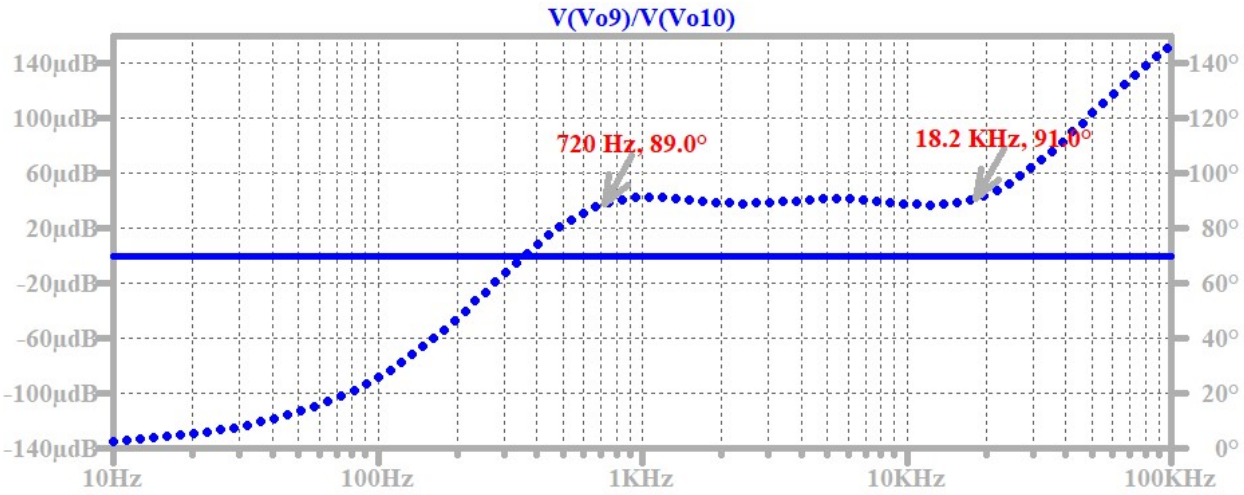

Figure 4: 5 Stage, 2.155 NtN Polyphase Filter Simulated Frequency Response, 10 Hz to 100 kHz

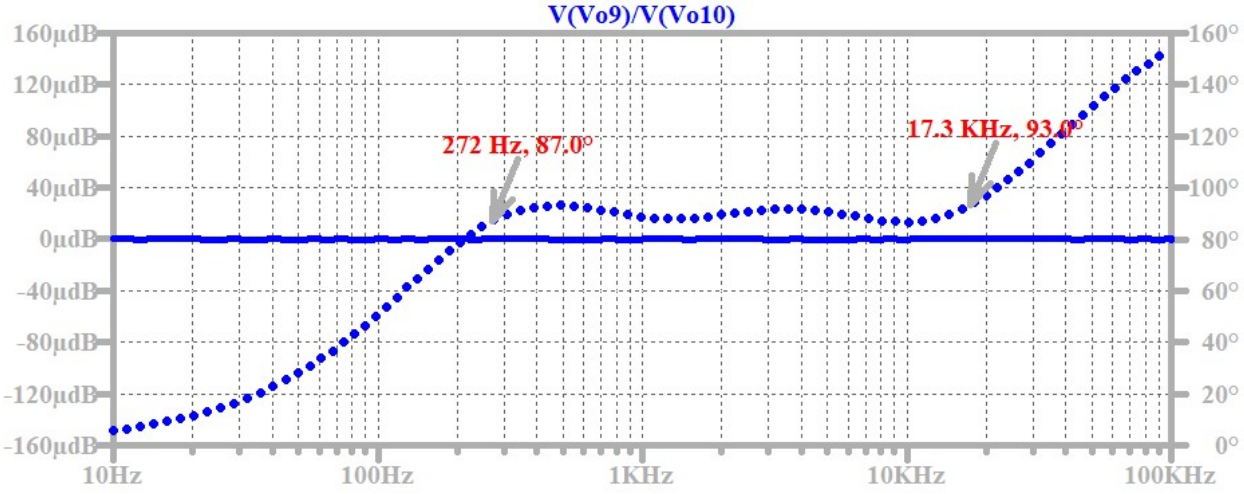

Figure 5: 5 Stage, 2.612 NtN Polyphase Filter Simulated Frequency Response, 10 Hz to 100 kHz

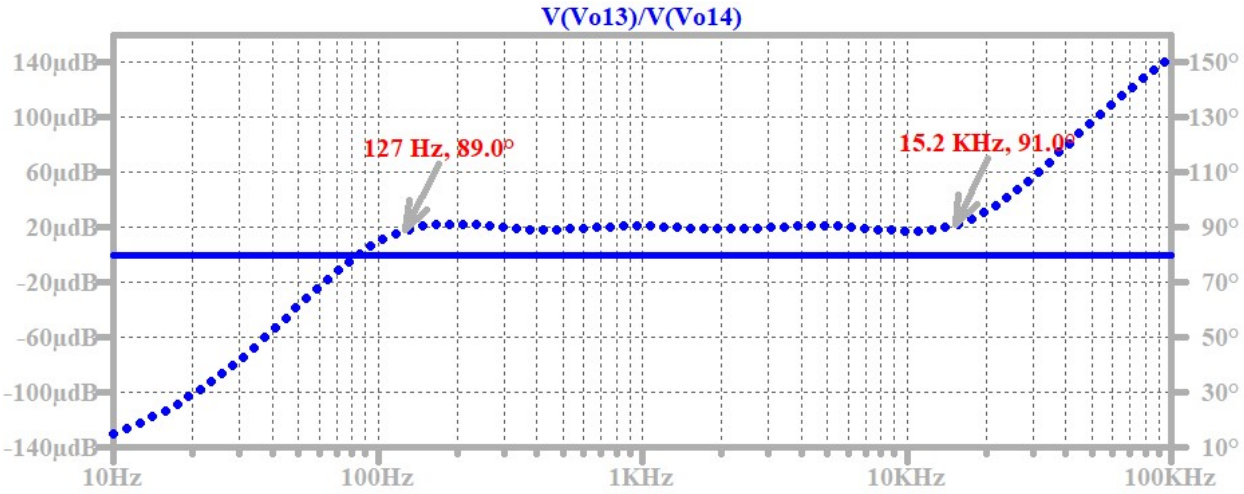

Figure 6: 7 Stage, 2.154 NtN Polyphase Filter Simulated Frequency Response, 10 Hz to 100 kHz

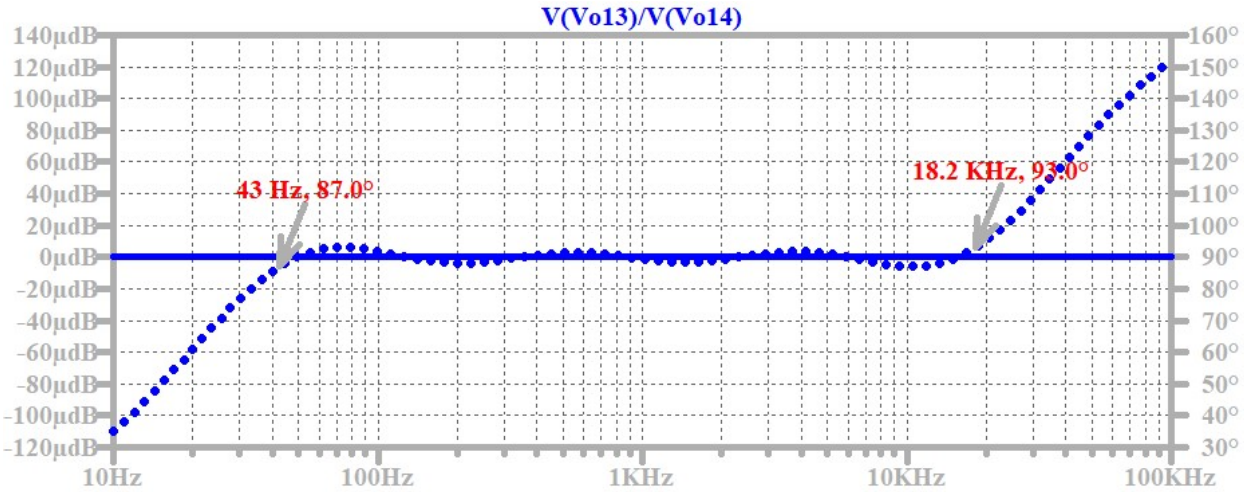

Figure 7: 7 Stage, 2.611 NtN Polyphase Filter Simulated Frequency Response, 10 Hz to 100 kHz

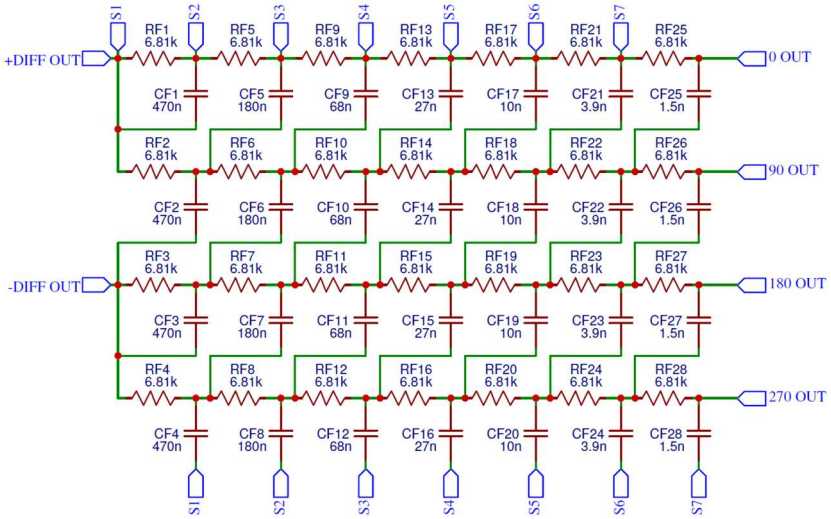

Figure 8: 7 Stage, 2.611 NtN Polyphase Filter Schematic Diagram

Differential Amplifier

As the Polyphase Filter required both the original signal and its inverse as inputs, the design process continued in the creation of signal inverter. Looking at single to differential ended signaling conversion methods due to differential signaling requiring accurate, well matched inverted signal pairs led to the rail-to-rail, fully differential amplifier. Compiling a list of options from part databases and comparing the varying performances of each chip resulted in the selection of the THS4531A. Implementing the basic design presented in [11] for an AC coupled single-differential ended signal converter in simulation alongside a SPICE model for the chip provided on the TI website produced the design shown in ***Figure 9***, with the component values chosen creating a wide passband extending well beyond both the upper and lower edges of the audio band. Further, the use of a 1x gain configuration avoided any possible distortion or loading effects from the large capacitive component of the Polyphase Filter.

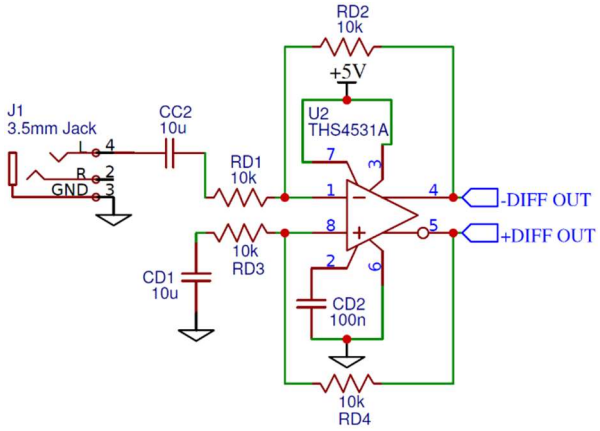

Figure 9: Initial Single-Differential Ended Amplifier Schematic Diagram

Buffer Amplifier

Since the Polyphase Filter chosen utilized a passive topology, it required buffer circuitry. To avoid any possible loading of the sensitive filter, the buffer amplifier required a high input impedance, unity gain stable rail-to-rail op-amp. With a nominal input impedance >1 TΩ, the LMC660/662 (quad/dual package) op-amp matched the requirements perfectly. ***Figure 10*** shows the quad pack LMC660 implemented alongside the four-output Polyphase Filter.

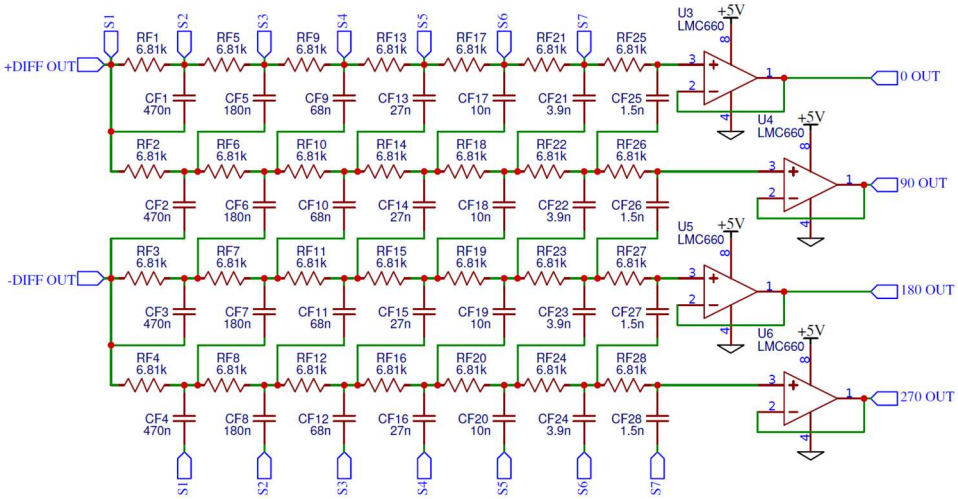

Figure 10: Polyphase Filter and Buffer Amplifier Schematic Diagram

Stereo Audio Power Amplifier

Due to the large loads in the range of 8Ω to 32Ω presented by speakers, any speaker-driving outputs required a power amplifier. Initially narrowing down the vast array of options to stereo amplifiers by deciding to limit the high-power outputs to the two-channel variable phase signals, the feasible options were further restricted to the subset of single-supply Class AB amplifiers and switching Class D amplifiers by the single-supply power system. Performing testing as described in **Testing & Construction** on a typical consumer electronic device such as a cellphone to measure the audio output voltage levels available produced the required output power range for the amplifier of 0.25W to 5W.

This power range eliminated most Class AB options which largely fell in the 0.1W to 0.2W range, and the lack of power efficiencies above 50% eliminated the rest. As such, the remaining options all consisted of Class D amplifiers utilizing a high frequency PWM switching modulation scheme to achieve vastly superior power efficiencies in the 85%-90% range. Though a wide variety of chips available satisfied the electrical needs of the amplifier, hand-soldered assembly prevented the use of any IC with a lead-less package or thermal ground pads, eliminating everything except for the Diodes Incorporated PAM series. Chosen due to its analog gain control, the 3W PAM8008 offered a more minimal control interface over the other models. Thus, the design from [12] in its entirety became the schematic in ***Figure 11,*** with the 100 nF, 1 µF, and 10 µF bypass capacitors omitted from schematic but used in the construction. This made the initial design exceedingly simple after component selection.

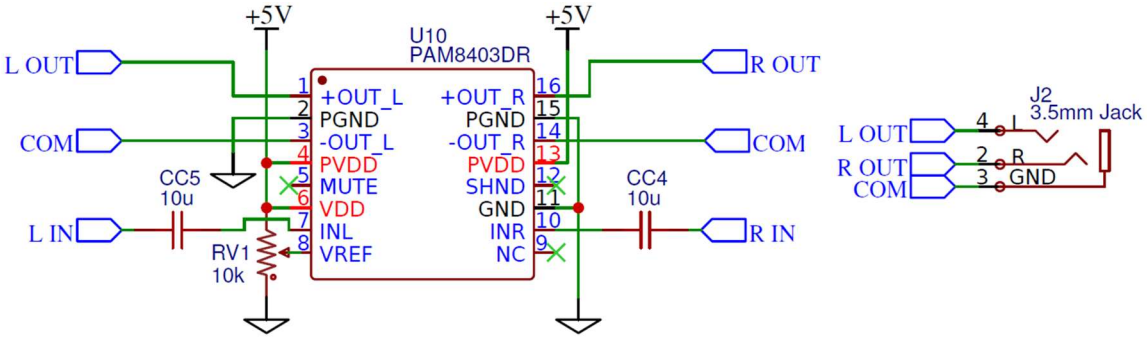

Figure 11: Initial Stereo Audio Power Amplifier Schematic Diagram

Two-Channel Phase Sum

Achieving the two-channel variable phase difference required a simple double summing junction between the buffered 0˚, 90˚, and 180˚ Polyphase Filter outputs. Easily implemented as a matched resistive sum, this system relied on a pair of variable resistances moving in sync with each other to correctly create the phase difference between the channels. As such, a dual digital potentiometer presented itself as the simplest solution. Choosing the AD5222 to avoid any noise from digital control circuitry, implementing its push-button interface proved straightforward. As seen below in ***Figure 12***, when the potentiometer wipers are shorted to B, both channels sit at 90˚ and are therefore 0˚ apart, while when the potentiometer wipers are shorted to A, the right channel becomes 0˚ while the left channel goes to 180˚, creating the maximum 180˚ difference desired. This passive summing network is also buffered by a pair of LMC662s, ensuring no loading effects.

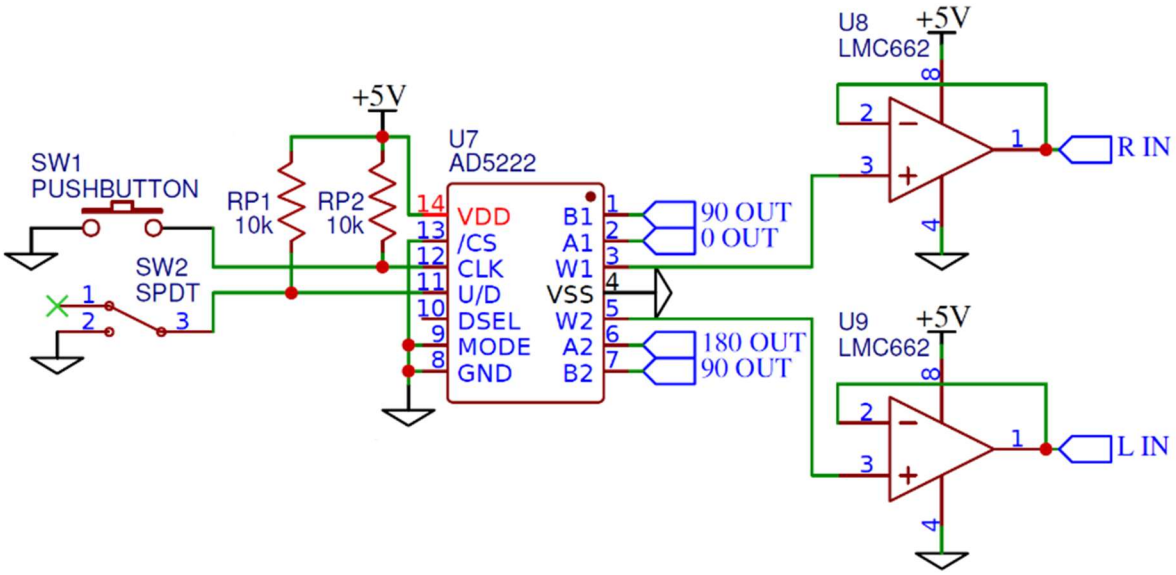

Figure 12: Two-Channel Phase Sum Schematic Diagram

Design Refinements

Due to issues uncovered during the testing of the initial design, the final design included two additional subsystems as seen in ***Figure 13*** and ***Figure 14***: the Amplitude Inverse Filter and the Common-Ground Averaging Network. This section describes the issues they address and the continued design process necessary for their creation.

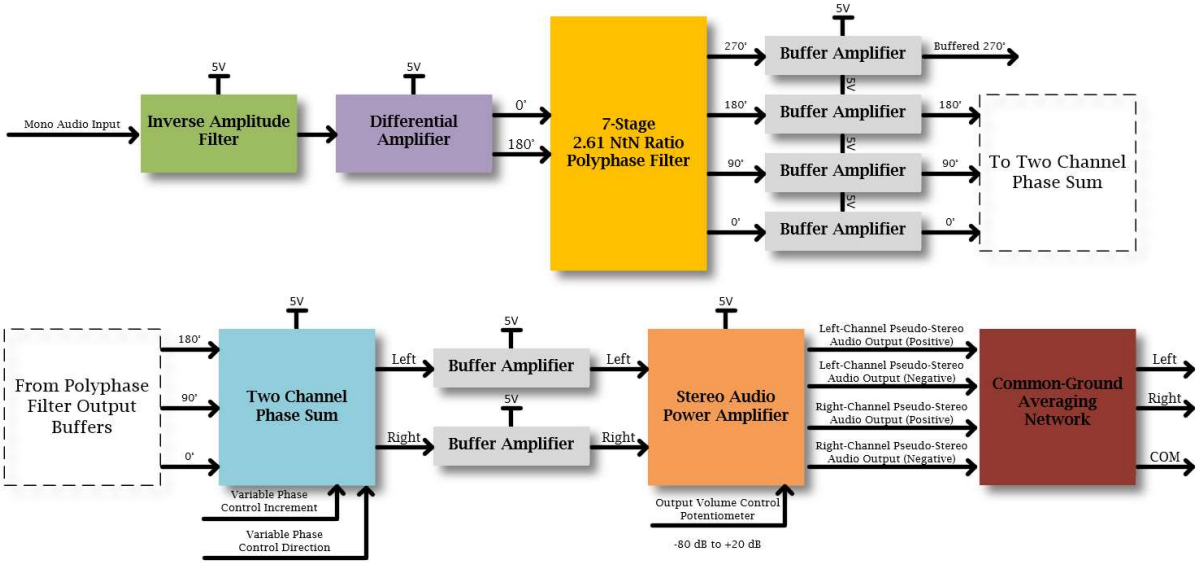

Figure 13: Final Design Sub-System Decomposition

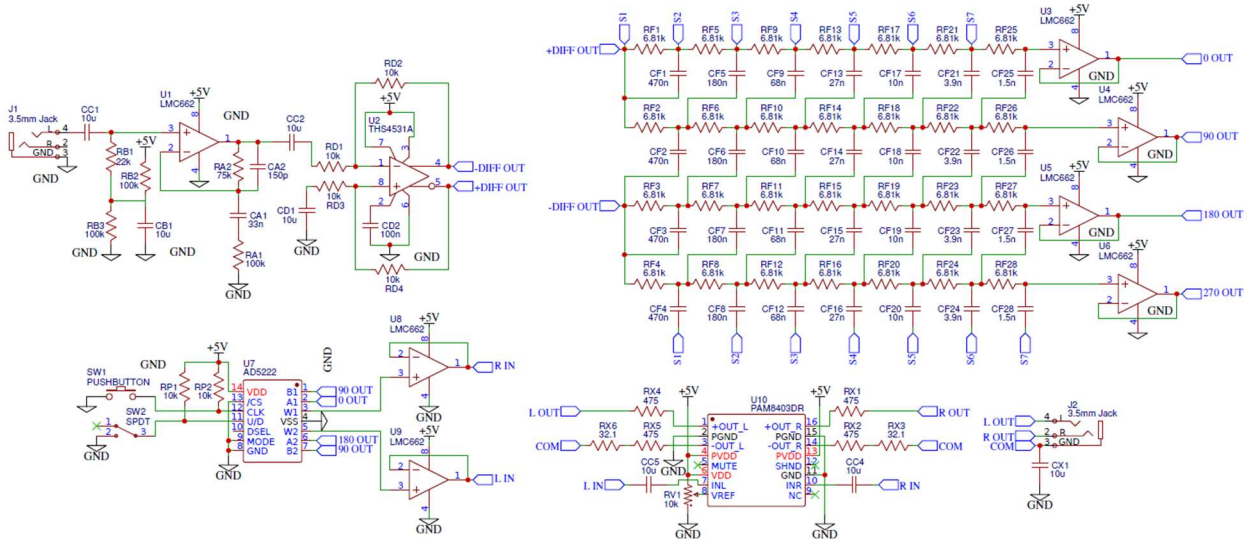

Figure 14: Final Full System Schematic Diagram

Amplitude Inverse Filter ($A^{-1}F$)

During full system listening tests, it became apparent that the parabolic, mid-band magnitude attenuation of the Polyphase Filter shown in ***Figure 18*** drastically reduced the listenability of any music, diminishing the volume of the main frequencies heard by human ears by as much as 5 dB. As such, the addition of an active band-pass filter tuned as the inverse of

the Polyphase Filter to the design served to augment the total frequency response, directly combating the attenuation. As seen in ***Figure 16***, the final design utilized a two pole, two zero buffered RC filter. Heuristically, the filter behavior consists of two superimposed effects: a 1 pole, 1 zero high-pass filter and a 1 pole, 1 zero low-pass filter. Since both component filters contain a pole and a zero, they each have two magnitude "states", one at the absolute value of the peak magnitude and one at unity gain. At frequencies between the pole and zero, they each transition from one state to the other.

Analytically, finding the filter transfer function involves applying Kirchhoff's Current Law and the Quadratic Formula to the generic schematic shown in ***Figure 15*** while assuming ideal op-amp properties as demonstrated below**.**

By KCL,

$$\frac{Vi-0V}{R1+\frac{1}{sC1}}=\frac{Vo-Vi}{R2||\frac{1}{sC2}},R2||\frac{1}{sC2}=\frac{R2}{R2C2s+1}\rightarrow Vo=\left(1+\frac{sC1(R2||\frac{1}{sC2})}{R1C1s+1}\right)Vi$$

$$\rightarrow\frac{Vo}{Vi}=H(s)=\left(1+\frac{R2C1s}{(R1C1s+1)(R2C2s+1)}\right)=\left(\frac{R1C1R2C2s^2+(R1C1+R2C2+R2C1)s+1}{R1C1R2C2s^2+(R1C1+R2C2)s+1}\right)$$

Using the Quadratic Formula and letting H(s) = N(s)/D(s),

$$For\ N(s),s=-\left(\frac{R1C1+R2C2+R2C1}{2R1C1R2C2}\right)\pm\sqrt{\left(\frac{R1C1+R2C2+R2C1}{2R1C1R2C2}\right)^2-\frac{1}{R1C1R2C1}}$$

Abstracting, let $A=\frac{R1C1+R2C2+R2C1}{2R1C1R2C2}$, $E=\frac{1}{R1C1R2C2}$, and $B=\sqrt{A^2-E}\rightarrow E=A^2-B^2\therefore s=-A\pm B$

$$For\ D(s),s=-\left(\frac{R1C1+R2C2}{2R1C1R2C2}\right)\pm\sqrt{\left(\frac{R1C1+R2C2}{2R1C1R2C2}\right)^2-\frac{1}{R1C1R2C1}}$$

Abstracting, let $C=\frac{R1C1+R2C2}{2R1C1R2C2}$ and $D=\sqrt{C^2-E}\rightarrow E=C^2-D^2\therefore s=-C\pm D$

$$\rightarrow H(s)=\frac{(s+A-B)(s+A+B)}{(s+C-D)(s+C+D)}=\frac{(A-B)(A+B)}{(C-D)(C+D)}\frac{\left(1+\frac{s}{\omega z1}\right)\left(1+\frac{s}{\omega z2}\right)}{\left(1+\frac{s}{\omega p1}\right)\left(1+\frac{s}{\omega p2}\right)}=\frac{E}{E}\frac{\left(1+\frac{s}{\omega z1}\right)\left(1+\frac{s}{\omega z2}\right)}{\left(1+\frac{s}{\omega p1}\right)\left(1+\frac{s}{\omega p2}\right)}$$

$$\therefore H(s)=\frac{\left(1+\frac{s}{\omega z1}\right)\left(1+\frac{s}{\omega z2}\right)}{\left(1+\frac{s}{\omega p1}\right)\left(1+\frac{s}{\omega p2}\right)}\ where\ \omega z1=A-B,\omega z2=A+B,\omega p1=C-D,\omega p2=C+D$$

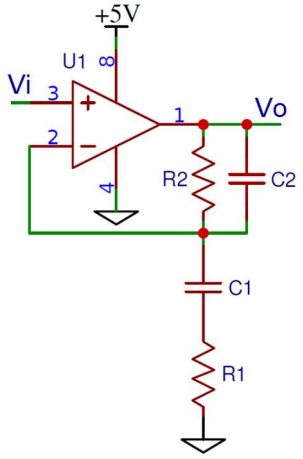

Figure 15: Generic Initial Amplitude Inverse Filter Schematic

After plotting the magnitude of the transfer function obtained above, the Solver function in Excel numerically evaluated possible combinations of component values pinning three points of the band-pass response to the desired inverse magnitude values from the Polyphase Filter until reaching an optimal solution. The three points chosen included the peak and the two points exactly 2 dB below the peak. However, due to the flat top response of the Amplitude Inverse Filter versus the parabolic shape of the Polyphase Filter, the undesired magnitude distortion could not be completely suppressed. Repeating the component optimization process until obtaining a well-optimized filter, the combined response of the final design exhibited less than 1 dB of total magnitude variation across the passband. ***Figure 17*** contains the theoretical magnitude response of the Amplitude Inverse Filter obtained directly from the transfer function and the final component values, while ***Figure 19*** contains the corresponding simulated response.

Though the Amplitude Inverse Filter design up to this point performed as desired in simulation, it required one further design change visible in the schematic. As the system used a single voltage rail, the AC-coupled input required some form of mid-rail bias network to avoid output clipping. Applying the bias circuit and some of the equations found in [10] quickly remedied this issue. Though this bias circuit slightly changed the frequency response, the general characteristics remained the same. ***Figure 20*** contains the total frequency response of the combined Amplitude Inverse Filter, Differential Amplifier, Polyphase Filter, and Buffer Amplifier signal path under an input amplitude of 2V to compensate for the flat 0.5x attenuation by the Differential Amplifier.

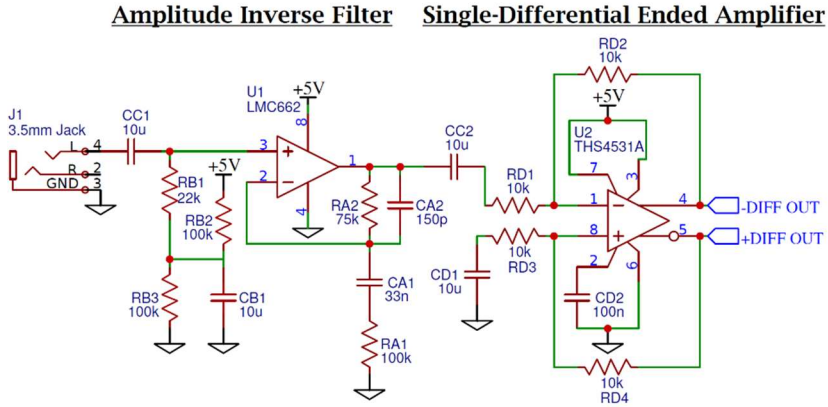

Figure 16: Final Pre-Amplifier Schematic Diagram

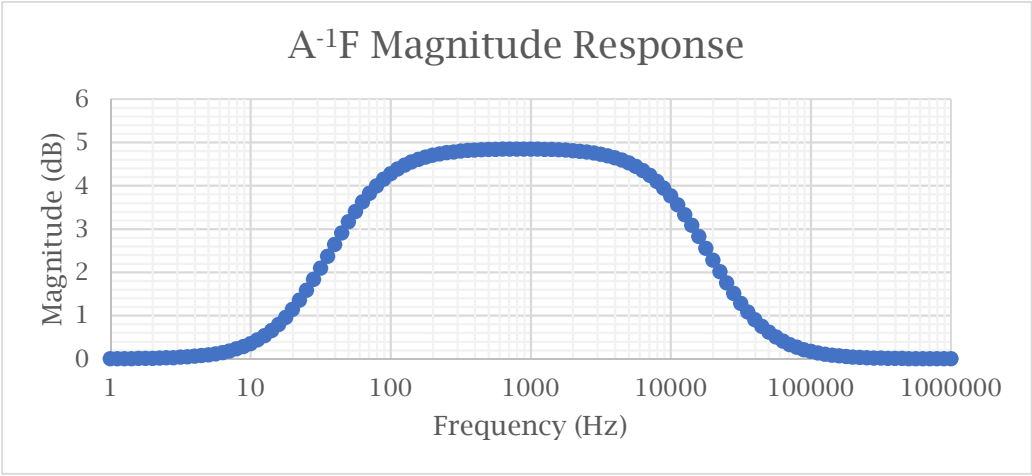

Figure 17: Amplitude Inverse Filter Theoretical Magnitude Response, 1 Hz to 1 MHz

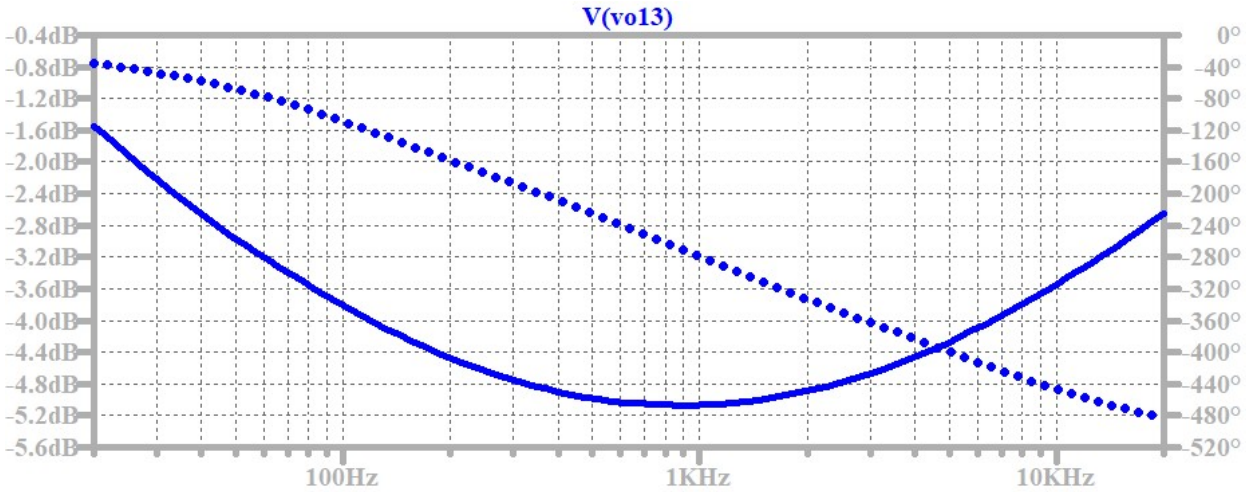

Figure 18: 7 Stage, 2.611 NtN Polyphase Filter Simulated Frequency Response, 20 Hz to 20 kHz

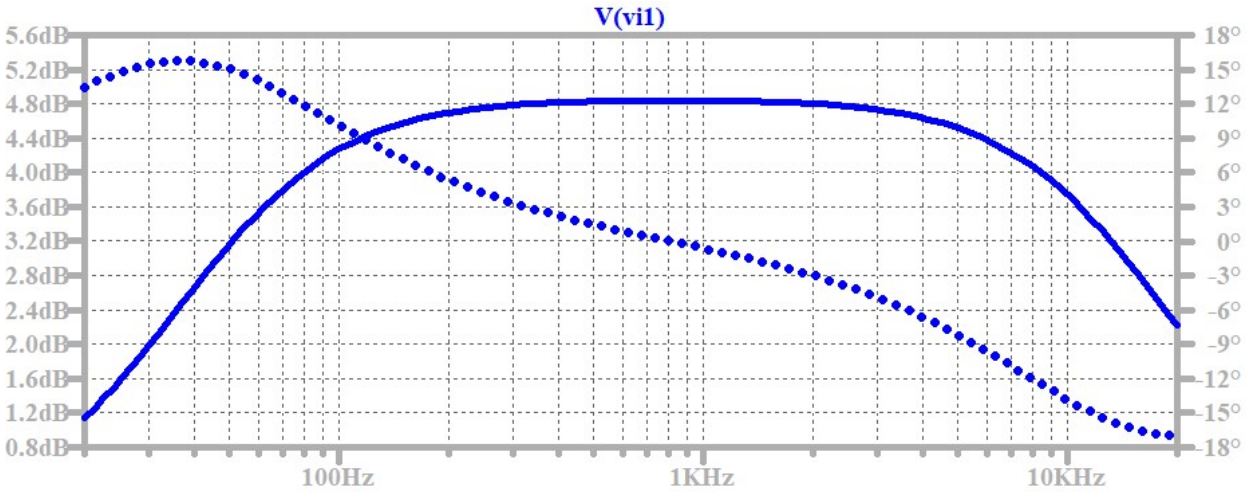

Figure 19: Amplitude Inverse Filter Simulated Frequency Response, 20 Hz to 20 kHz

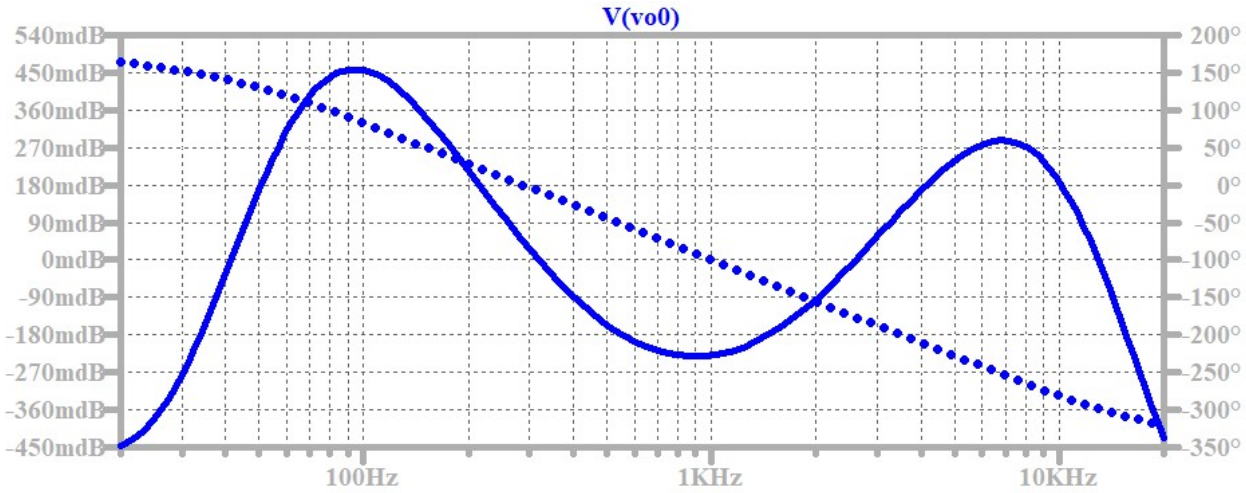

Figure 20: Simulated System Frequency Response, 20 Hz to 20 kHz

Common-Ground Averaging Network

As each subsystem's design, assembly, and test cycles occurred separately, a major issue with the output stage went unnoticed until the beginning of the complete system assembly. To avoid the need for large AC decoupling capacitors on the output lines to eliminate any DC bias across the speakers driven, all the Class D amplifiers examined as part of the Stereo Power Amp design process utilize differential outputs with a full H-bridge to perform the output switching. Since the common 3.5mm connector uses single-ended outputs sharing a common ground, shorting both negative channels to the common ground would have resulted in massive current spikes between the outputs, destroying the chip. With assistance from the project advisor, the creation of the averaging network seen in the final design of ***Figure 21*** served as a simple differential-single ended connector. Though an easily implemented passive network, any mismatch in branch resistance resulted in crosstalk between the channels, where components of one signal appeared in the other. This was especially prevalent at smaller branch resistance values, where a slight difference constitutes a larger error. As such, much of the design process consisted of iterative two-tone listening tests to find an acceptable balance between minor crosstalk and maximum output volume. Though attempted, the difficulty in accurately measuring the crosstalk between the switching outputs of the Class D made quantitative tests much more efficient.

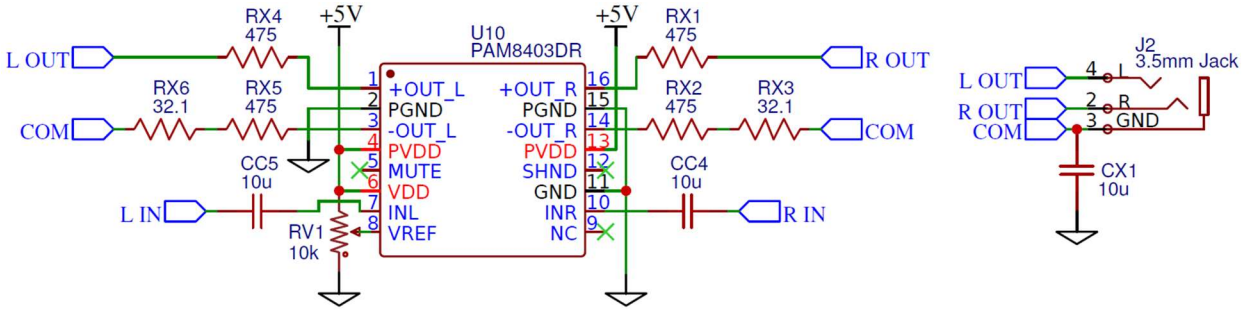

Figure 21: Final Output Stage Power Amplifier Schematic Diagram

Testing & Assembly

Due to the modular approach performed with most of the design, the organization of the following tests follows the subsystem approach used previously unless otherwise noted.

Amplitude Inverse Filter

The experimentally measured frequency response of ***Figure 22*** and ***Figure 23*** verify the behavior of the Amplitude Inverse Filter predicted in simulation.

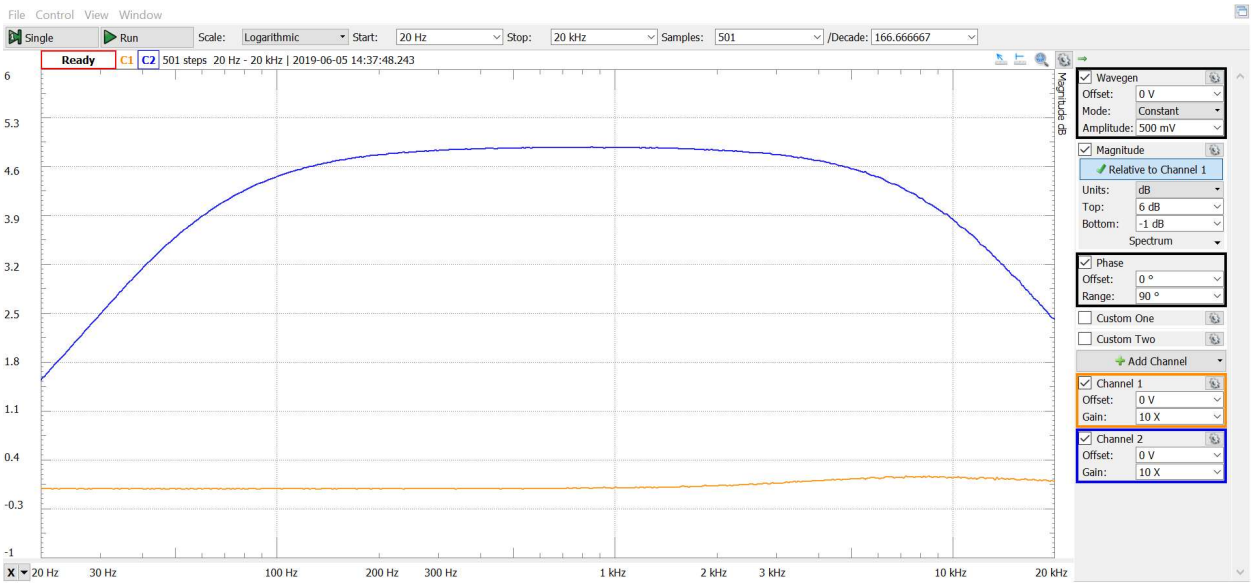

Figure 22: Normalized Experimental Magnitude Response of the Amplitude Inverse Filter

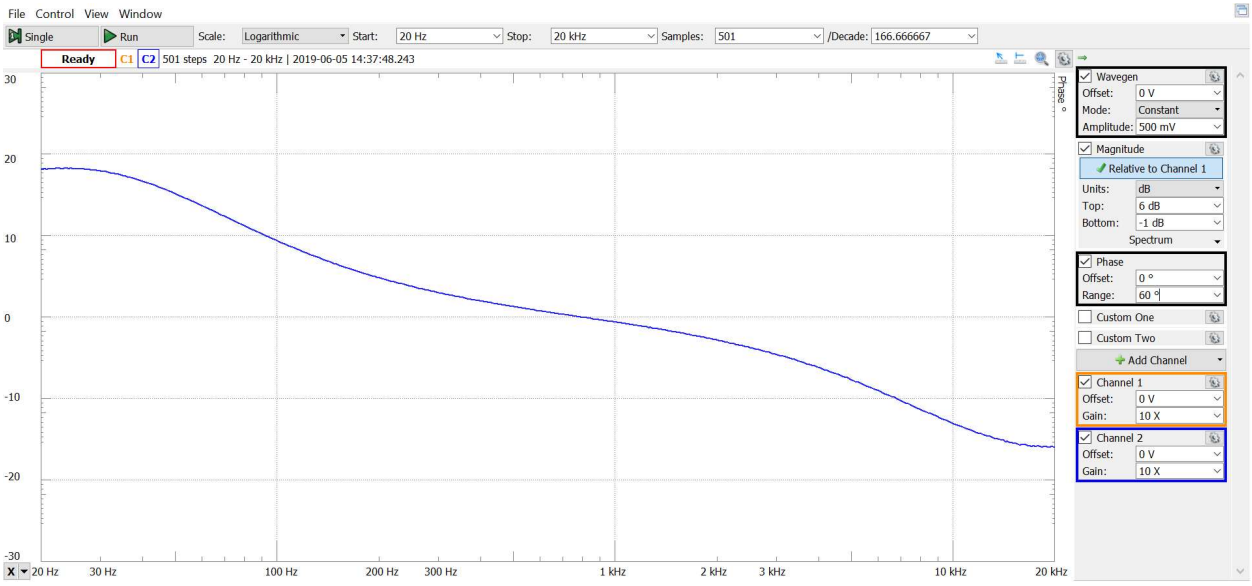

Figure 23: Normalized Experimental Phase Response of the Amplitude Inverse Filter

Differential Amplifier

The time-domain plot of ***Figure 24*** verifies the correct operation of the single-differential ended signal conversion by the Differential Amplifier, while the frequency response plot of ***Figure 25*** highlights the flat 6 dB signal attenuation caused by the conversion.

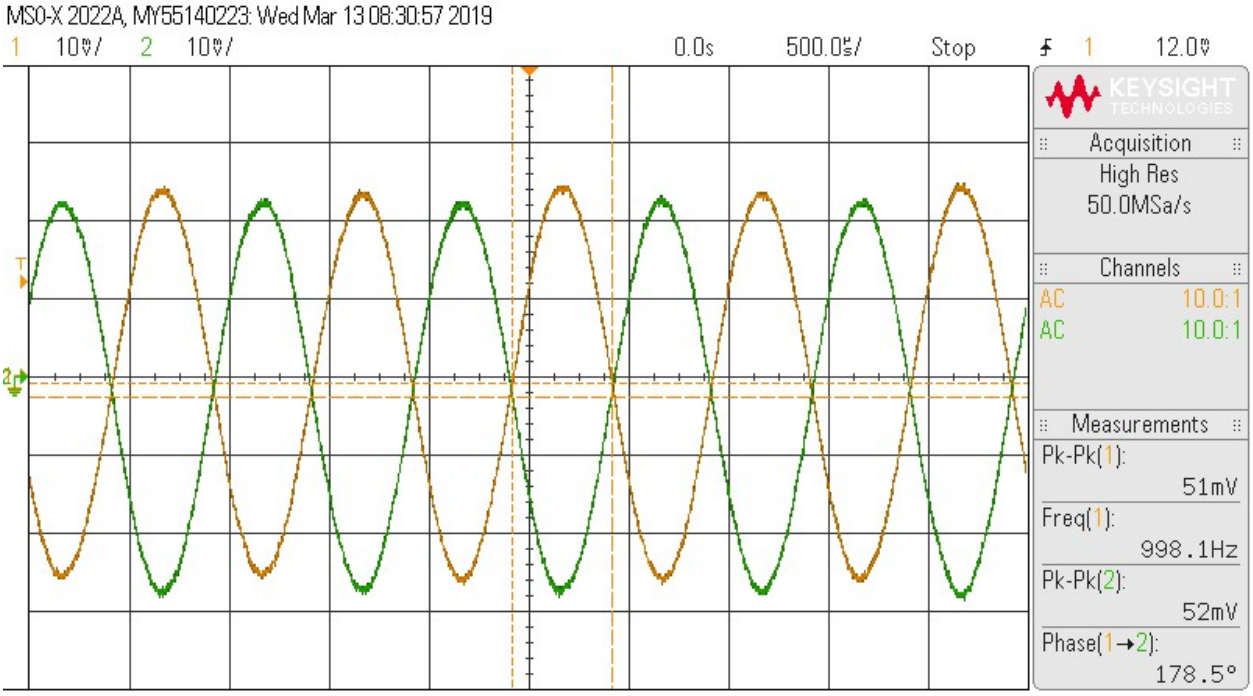

Figure 24: Time-Domain Differential Amplifier Output, f_{In} = 1kHz, V_{In} = 0.1V_{P-P}

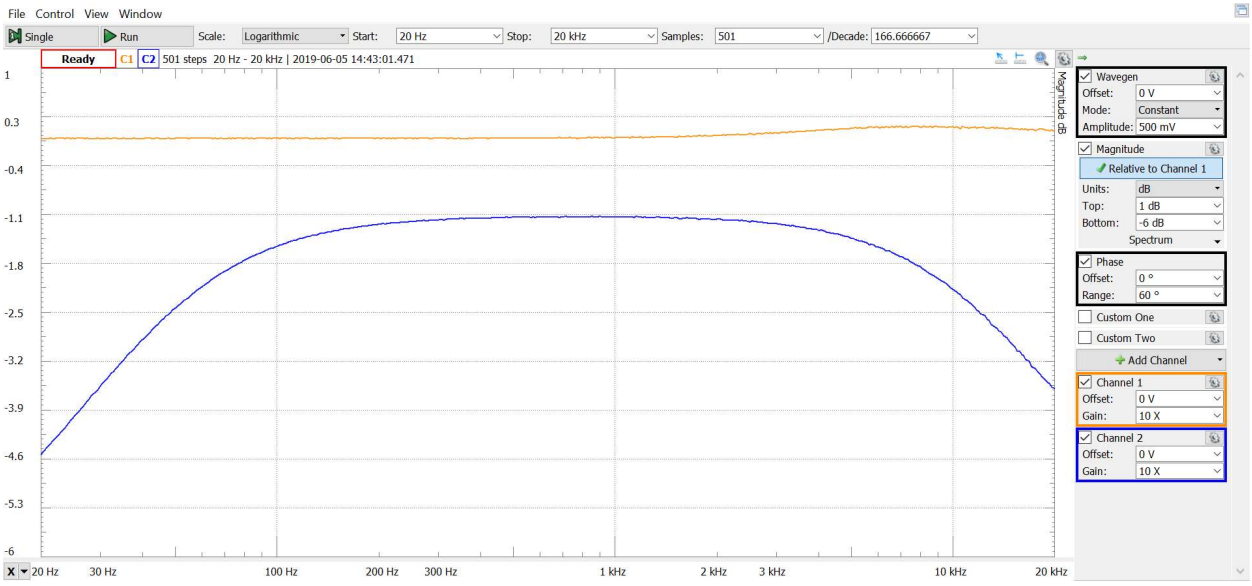

Figure 25: Normalized Experimental Magnitude Response of the Overall Pre-Amplifier

Stereo Audio Class D Power Amplifier

Though examining the high frequency switching waveforms directly provides little usable information about the input signal, it does provide information on the modulation pattern used. To avoid the large opposing source and sink currents required by a conventional differential signal, the Class D amplifier instead switches one side of the H-bridge slightly out of phase with the other as seen in ***Figure 26.*** Highlighted in ***Figure 27*** and ***Figure 28,*** the width of this phase variation directly corresponds to the amplitude of the input signal.

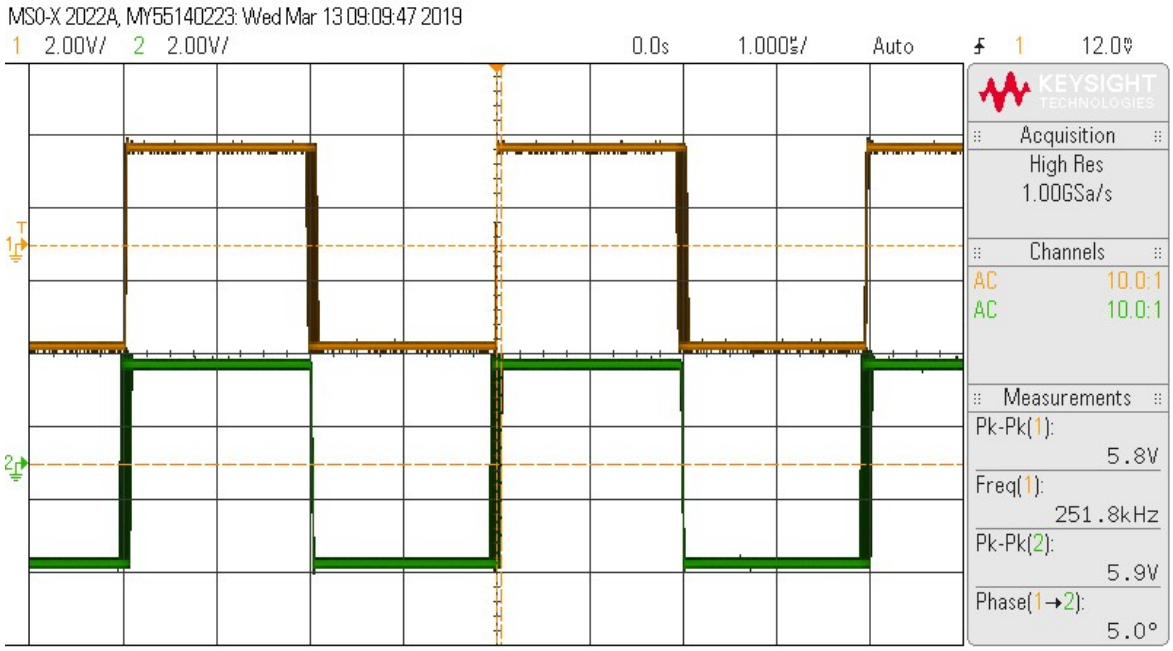

Figure 26: PAM8008 Class D +-ROut, 10kHz 1Vpp In - Full Wave

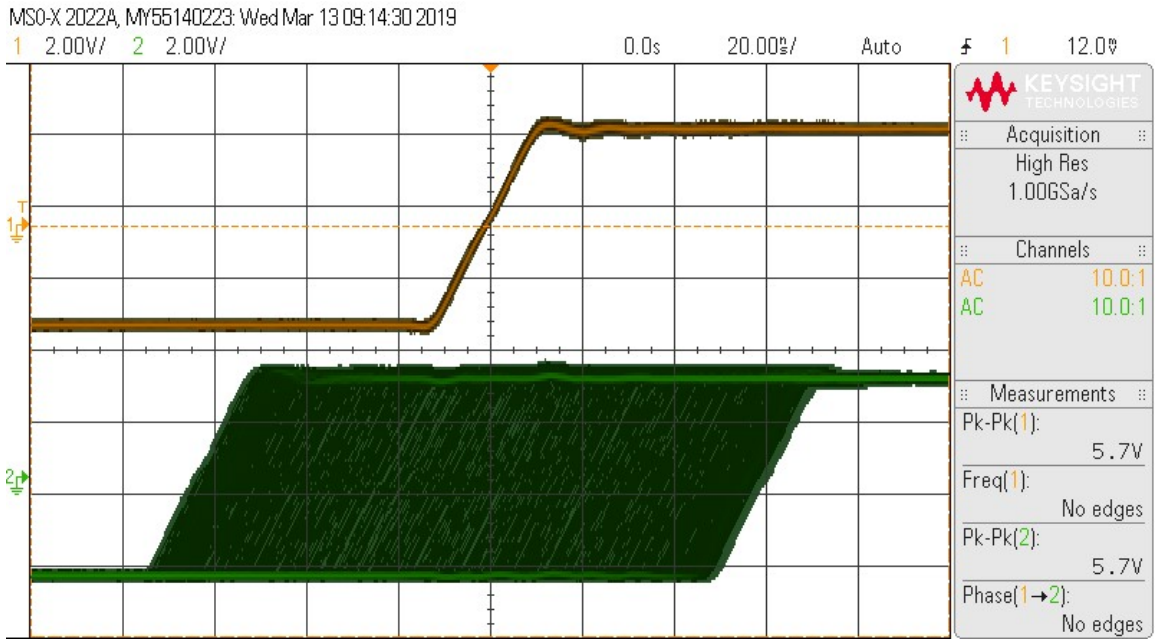

Figure 27: PAM8008 Class D +-ROut, 10kHz 1Vpp In – Persist

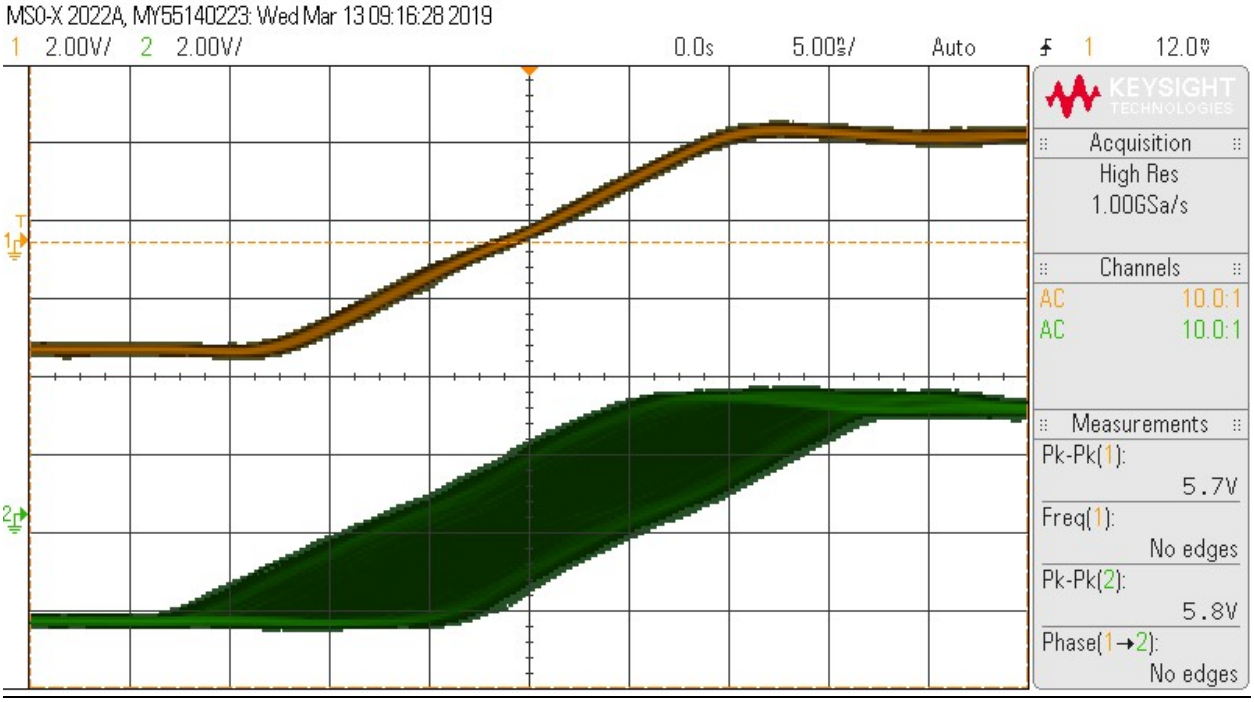

Figure 28: PAM8008 Class D +-ROut, 10kHz 100mVpp In - Persist

Shown below in ***Figure 29*** and ***Figure 30***, attempts to measure the crosstalk created by the addition of the Common-Ground Averaging Network while triggering the oscilloscope on the input waveform met mixed results. Though the desired output waveform could be consistently captured, the visual results exhibited much more crosstalk than the audible tests. This is likely due to the single-ended measurement performed on a differential output, as the ungrounded COM line connected to the negative terminal of each headphone driver moves slightly with the averaged combination of the left and right negative channels.

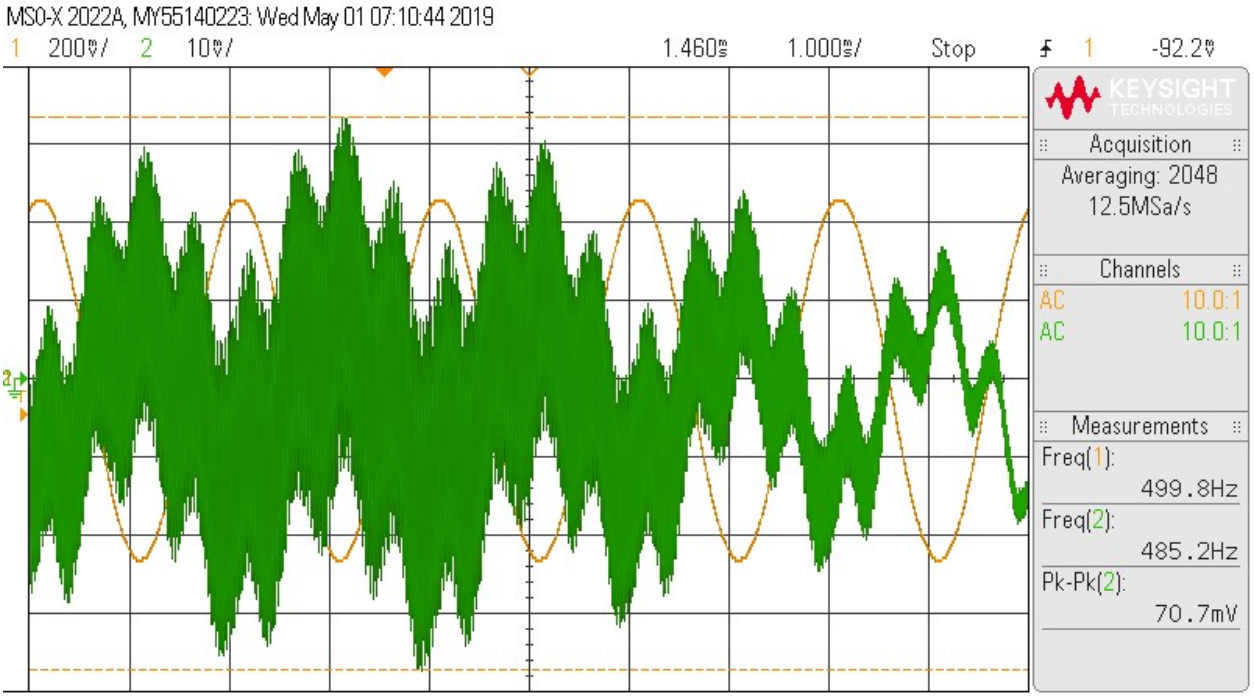

Figure 29: Class D Right I/O+, 500 Hz, 2kHz, 1Vpp In; 507.1 Ω Branch Resistance

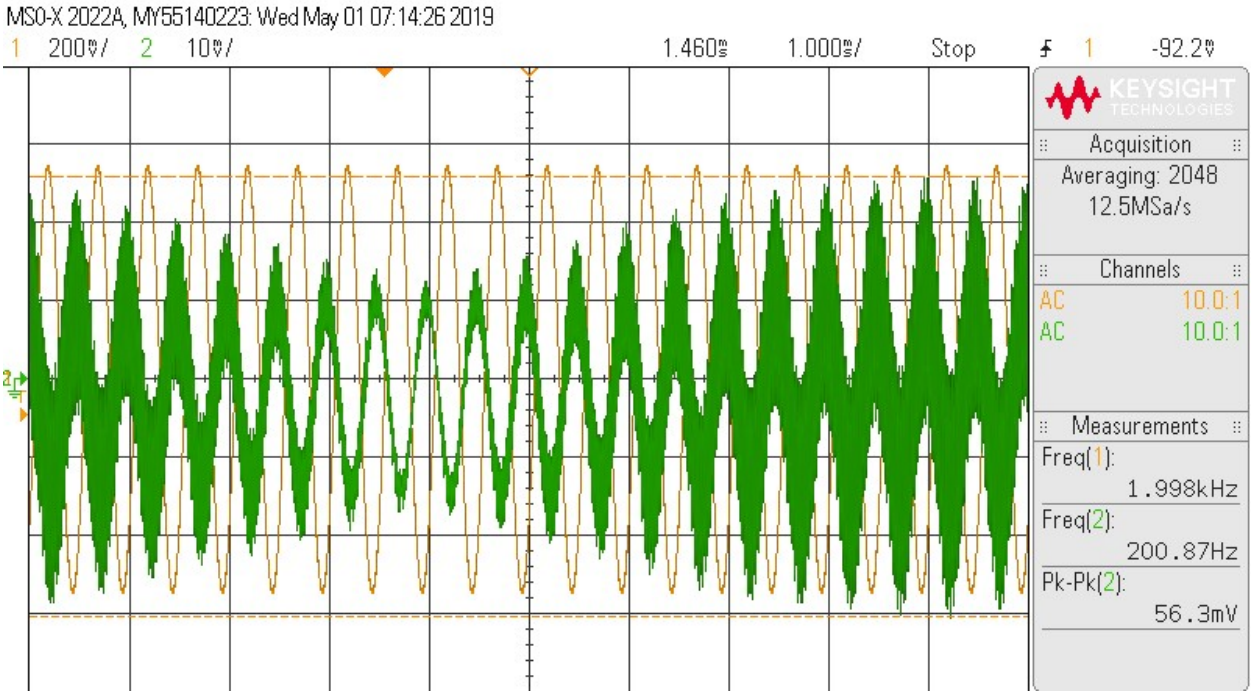

Figure 30: Class D Left I/O+, 500 Hz, 2kHz, 1Vpp In; 507.1 Ω Branch Resistance

System Tests

As each Polyphase Filter would require an Amplitude Inverse Filter tuned specifically for it, any system data which includes test cases for all four filters does not include the influence of the Amplitude Inverse Filter.

One-Tone Test Harmonic Spectrum Data

As an audio system, a broadband test such as a one-tone test provides experimental distortion data by showcasing the magnitude of each harmonic as well as the strength of the fundamental tone. ***Figures 31-34*** contain one-tone test Fast-Fourier Transforms for the full system connected to each Polyphase Filter built. Though performed with a tone amplitude well below the full voltage range of the system, these results correspond to a typical mid-volume use case. Thus, as the attenuation of all harmonics exceeds 40 dB for each filter case, these tests illustrate the desired low system distortion.

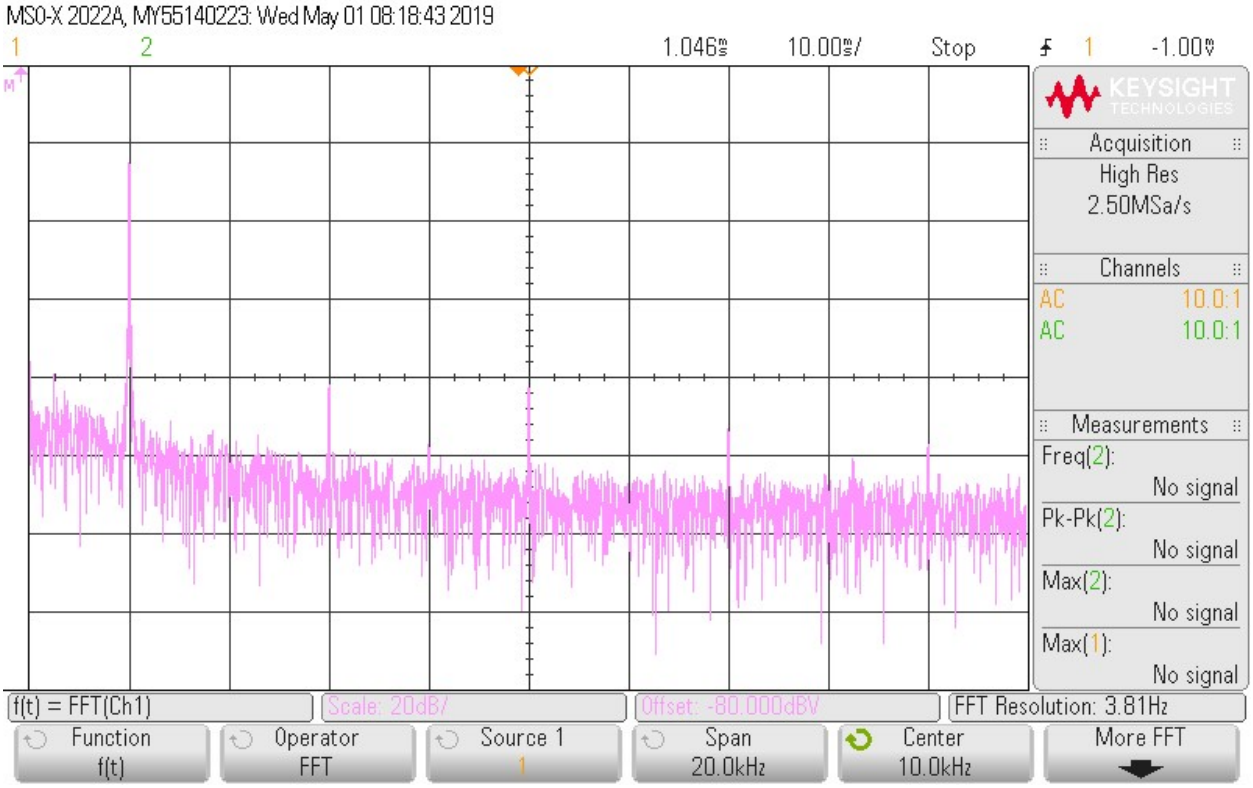

Figure 31: 5 Stage, 2.155 NtN PPF System One Tone Test FFT, f_{In} = 2kHz, V_{In} = 0.5V_{P-P}

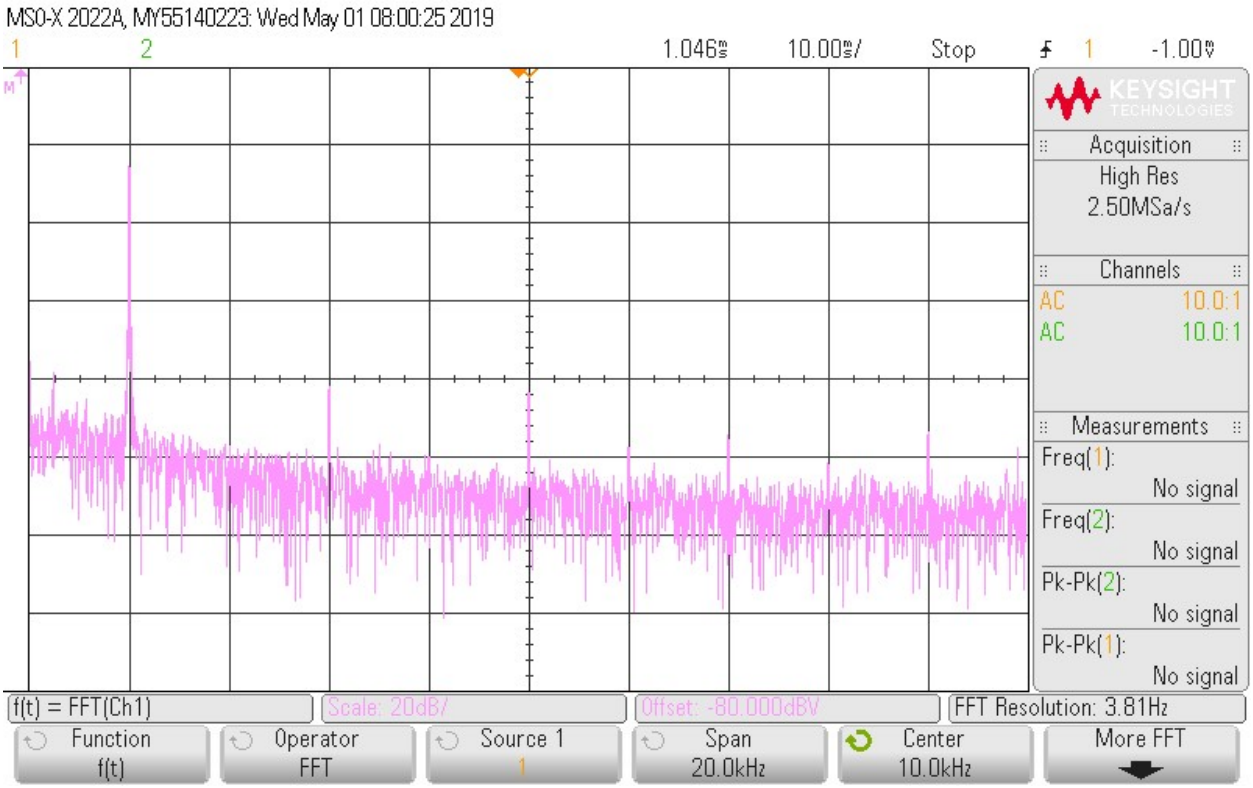

Figure 32: 5 Stage, 2.612 NtN PPF Full System One Tone Test FFT, f_{In} = 2kHz, V_{In} = 0.5V_{P-P}

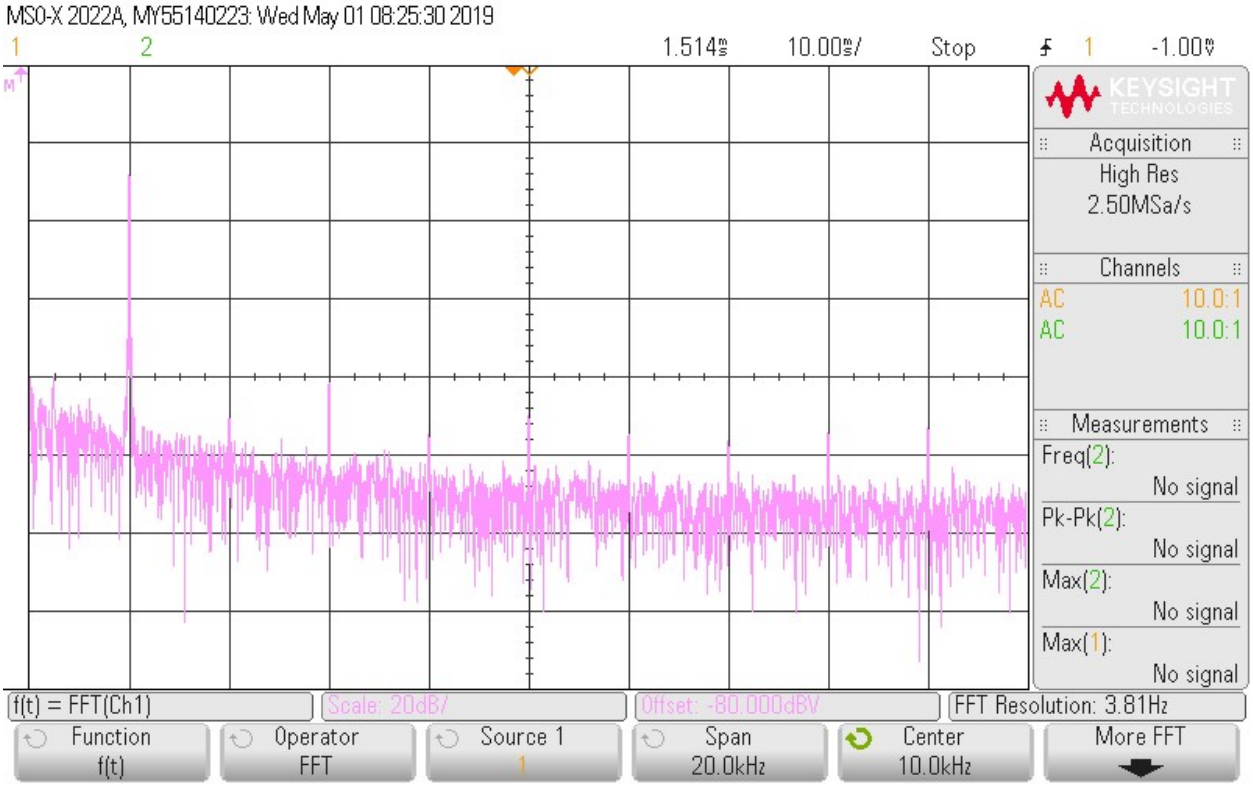

Figure 33: 7 Stage, 2.154 NtN PPF Full System One Tone Test FFT, f_{In} = 2kHz, V_{In} = 0.5V_{P-P}

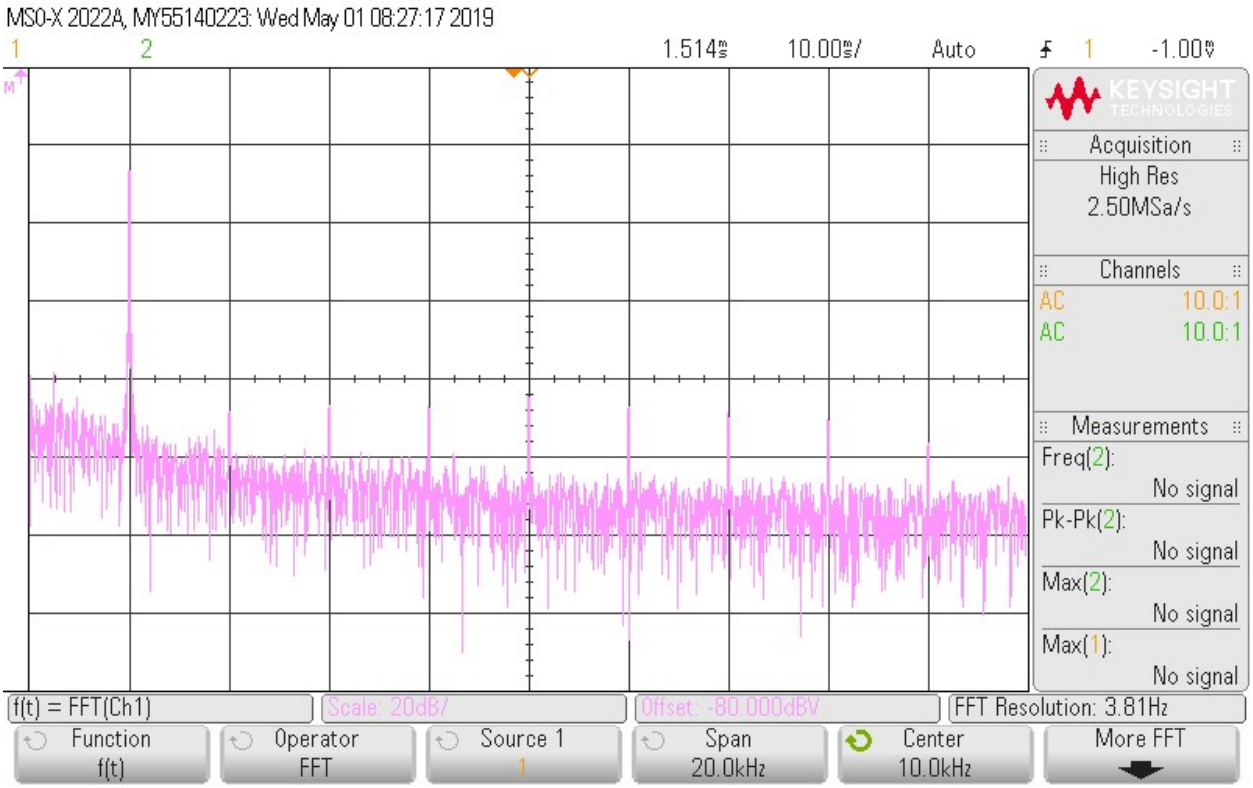

Figure 34: 7 Stage, 2.611 NtN PPF Full System One Tone Test FFT, f_{In} = 2kHz, V_{In} = 0.5V_{P-P}

X-Y Domain Oscilloscope Captures

Similar to the one-tone test data, each X-Y capture in ***Figures 35-38*** corresponds to a unique Polyphase filter connected to the system. The 0˚ and 90˚ Buffer Amplifier outputs provided the image data. As each filter produced a relatively uniform circle, this indicates that the phase separation at the testing frequency of 1 kHz is relatively consistent from filter to filter.

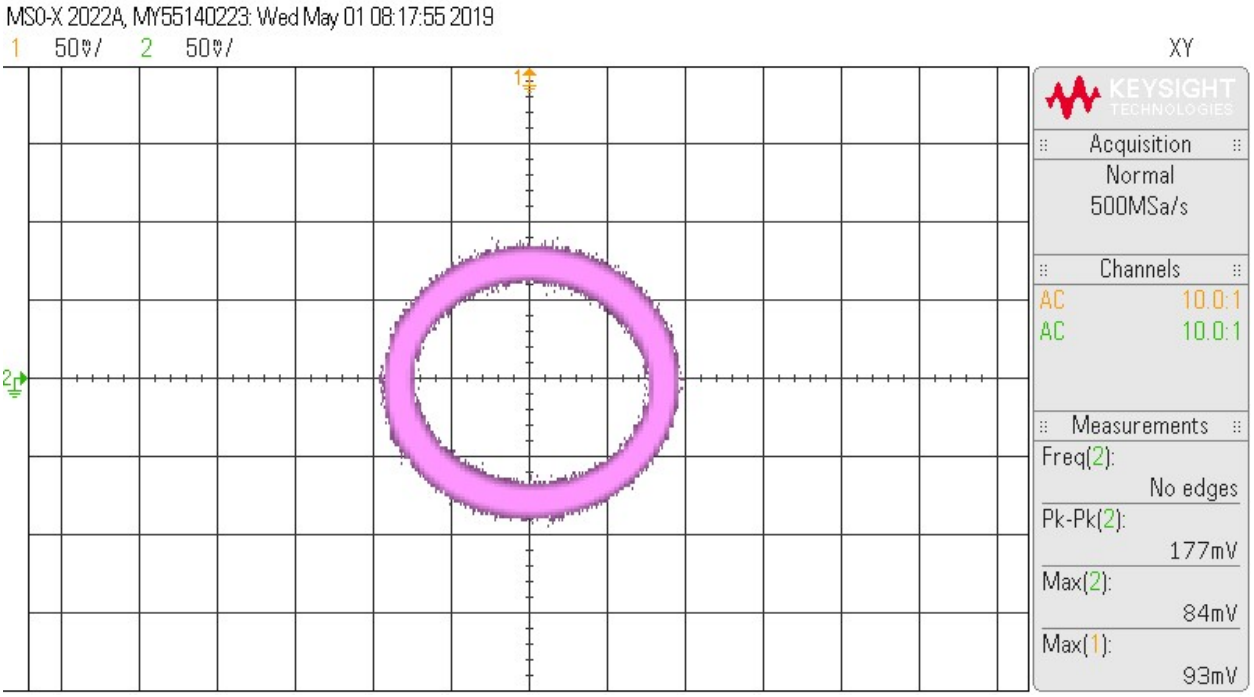

Figure 35: 5 Stage, 2.155 NtN PPF Post-Buffer Amp 0˚, 90˚ XY Capture, f_{In} = 1kHz, V_{In} = 0.5V_{P-P}

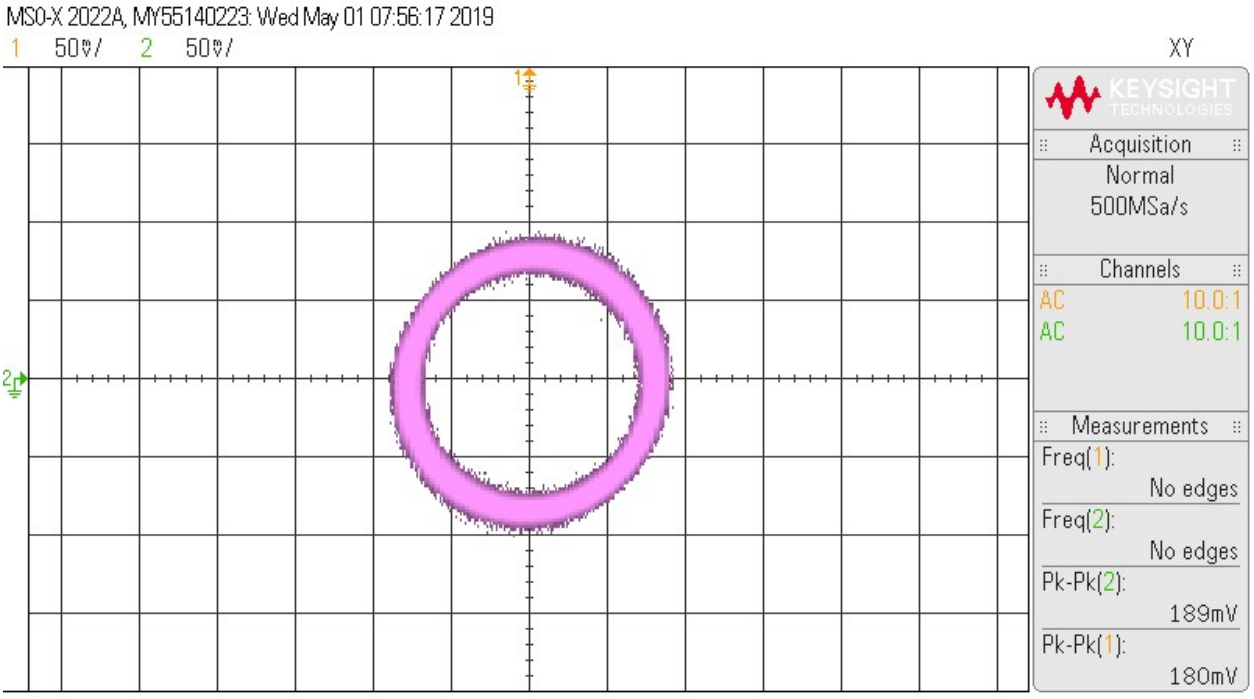

Figure 36: 5 Stage, 2.612 NtN PPF Post-Buffer Amp 0˚, 90˚ XY Capture, f_{In} = 1kHz, V_{In} = 0.5V_{P-P}

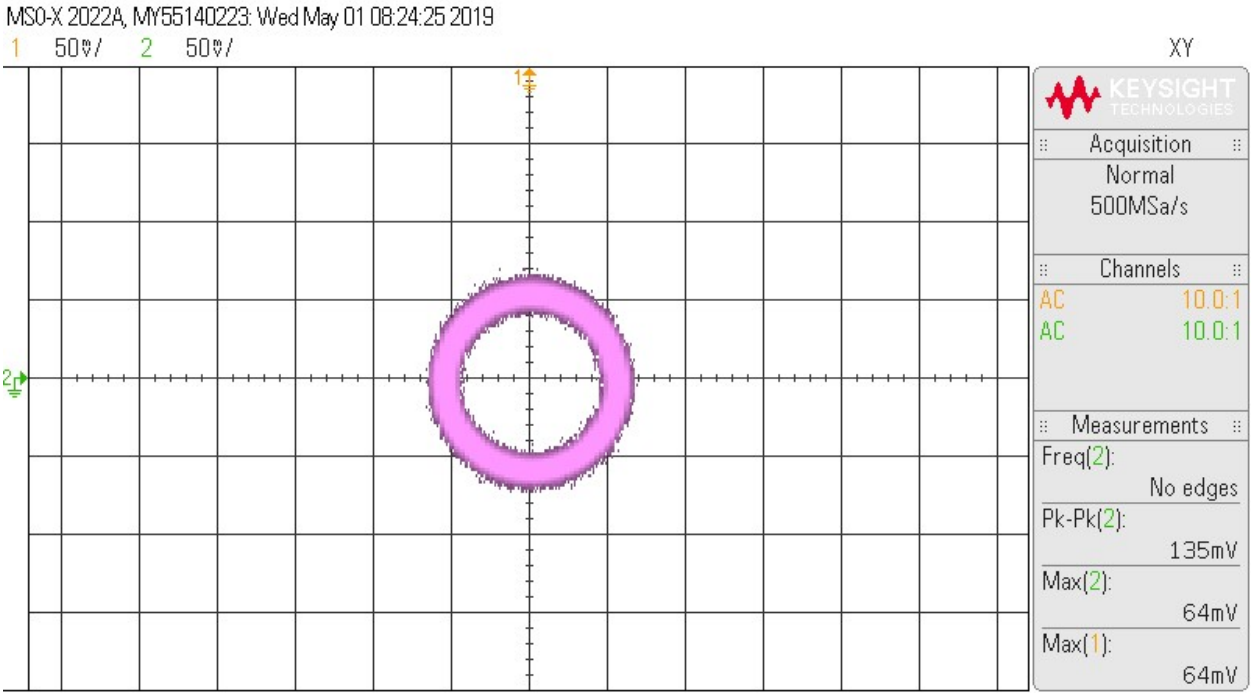

Figure 37: 7 Stage, 2.154 NtN PPF Post-Buffer Amp 0˚, 90˚ XY Capture, f_{In} = 1kHz, V_{In} = 0.5V_{P-P}

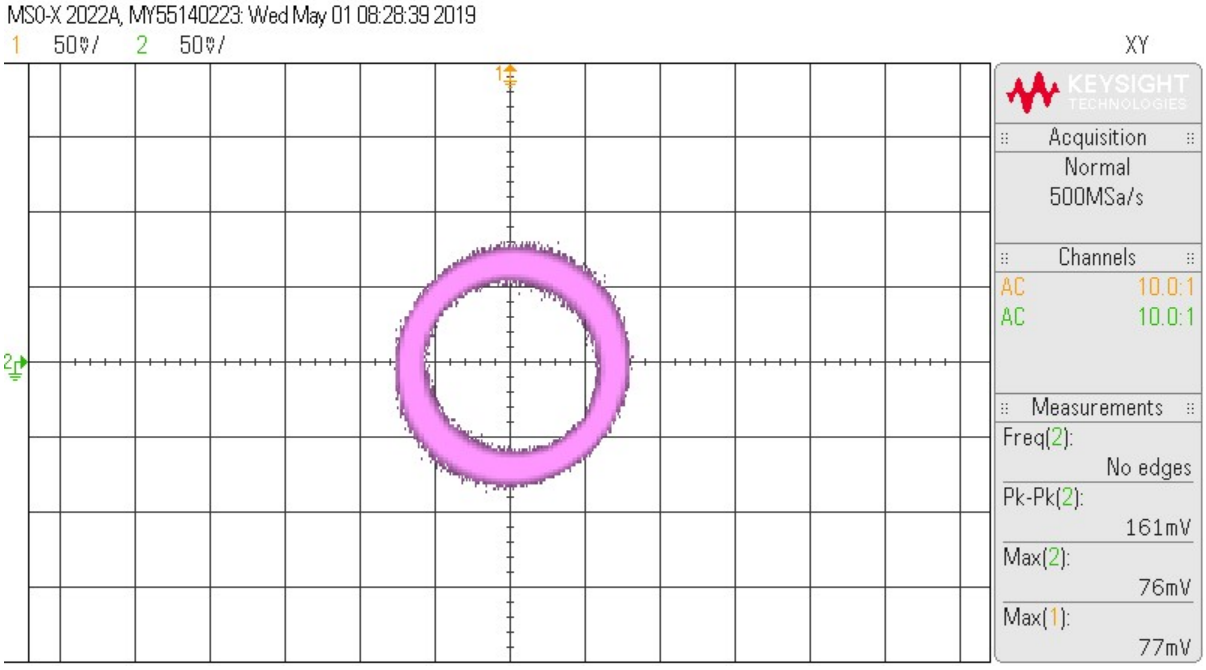

Figure 38: 7 Stage, 2.611 NtN PPF Post-Buffer Amp 0˚, 90˚ XY Capture, f_{In} = 1kHz, V_{In} = 0.5V_{P-P}

Quadrature Time-Domain Oscilloscope Captures

This series of time-domain oscilloscope captures in ***Figures 39-42*** showcase the buffered quadrature phase outputs of each Polyphase Filter. The important information presented in these images is that the amplitude and DC average of each wave roughly matches the out of phase copies, and that the phase differences are close to quadrature. Though these measurements seem the indicate phase variations larger than expected, this is simply an artifact of the inaccurate trigger mechanism of the four-channel oscilloscope used.

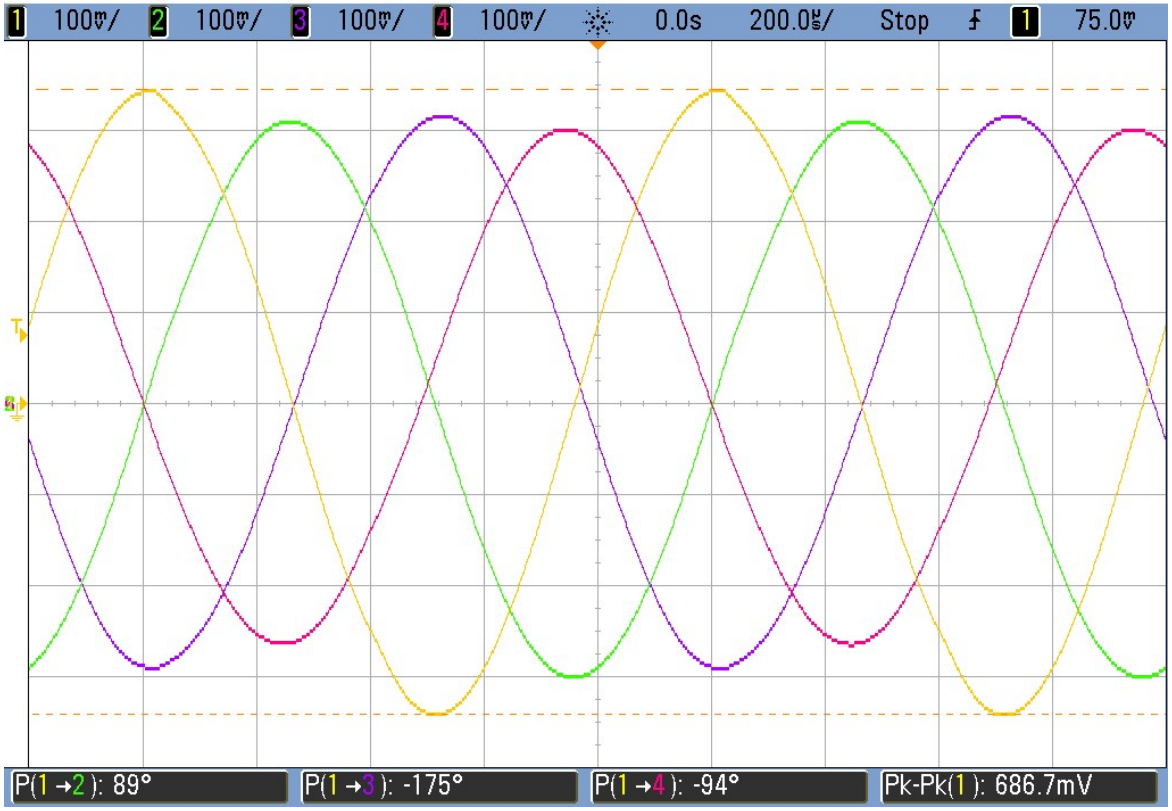

Figure 39: 5 Stage, 2.155 NtN PPF Post-Buffer Quadrature T-D Capture, f_{In} = 1kHz, V_{In} = $2V_{P-P}$

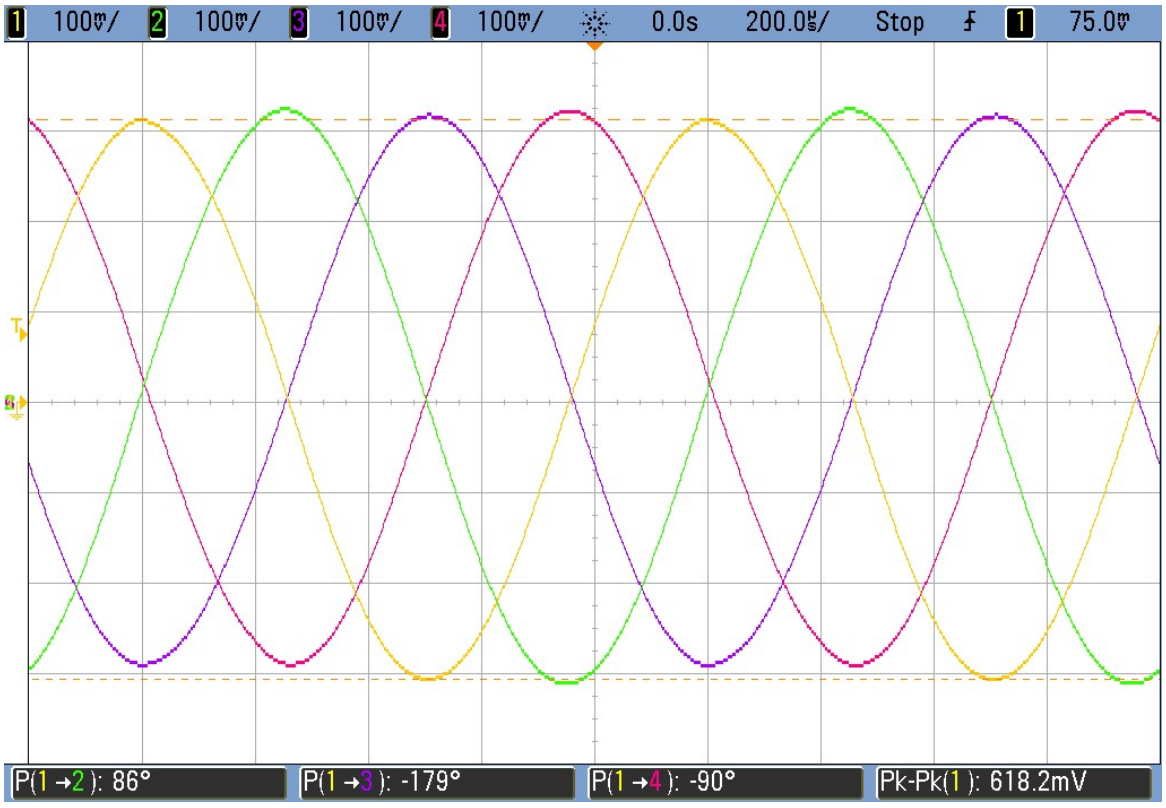

Figure 40: 5 Stage, 2.612 NtN PPF Post-Buffer Quadrature T-D Capture, f_{In} = 1kHz, V_{In} = $2V_{P-P}$

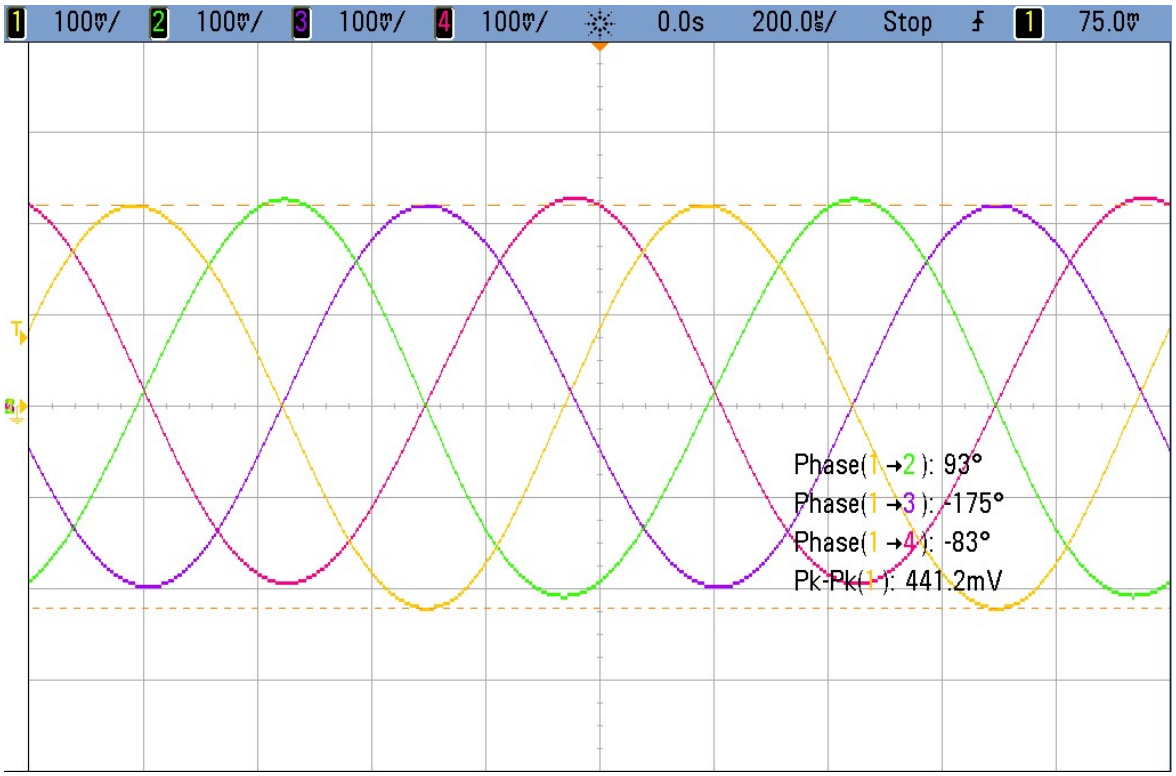

Figure 41: 7 Stage, 2.154 NtN PPF Post-Buffer Quadrature T-D Capture, f_{In} = 1kHz, V_{In} = $2V_{P\text{-}P}$

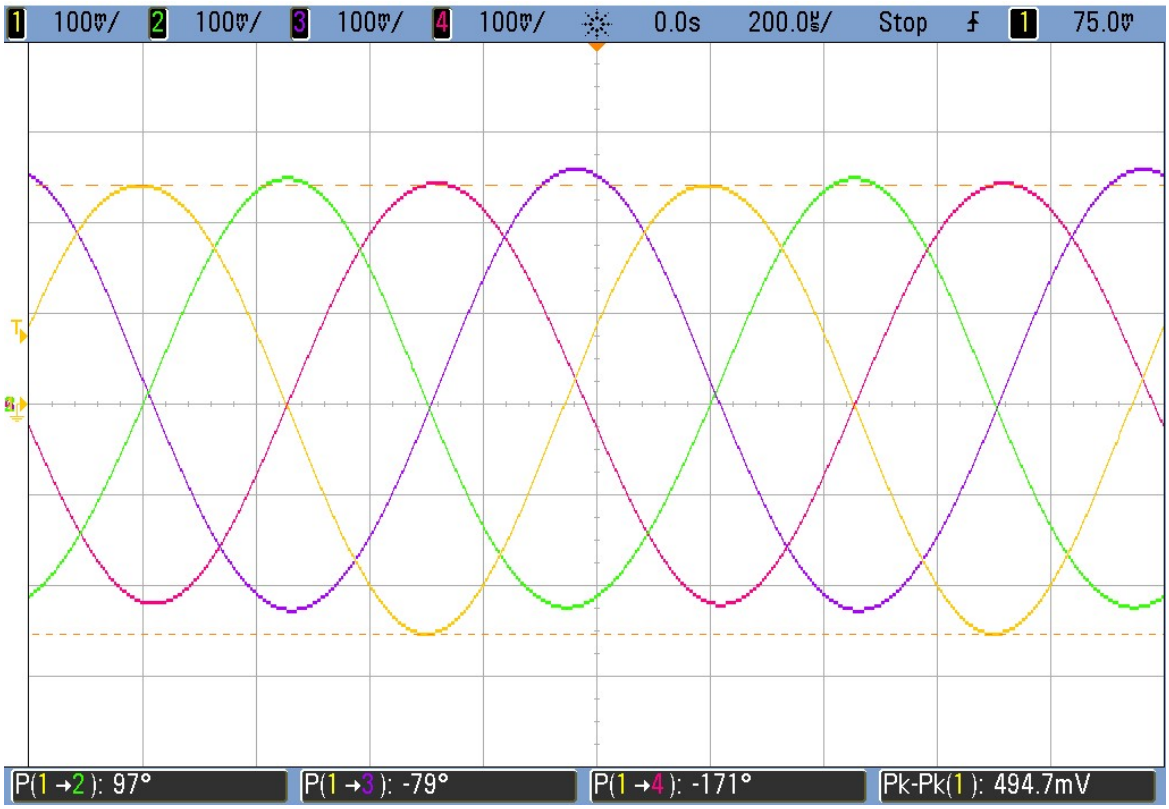

Figure 42: 7 Stage, 2.611 NtN PPF Post-Buffer Quadrature T-D Capture, f_{In} = 1kHz, V_{In} = $2V_{P\text{-}P}$

Variable Phase Channel Separation

Implemented last, the variable phase outputs were only tested with the seven stage Polyphase Filter used in the final design. ***Figures 43-45*** show that the system variable phase outputs approach the full separation range edges of 0˚ and 180˚ as expected and precise intermediary points such as 90˚.

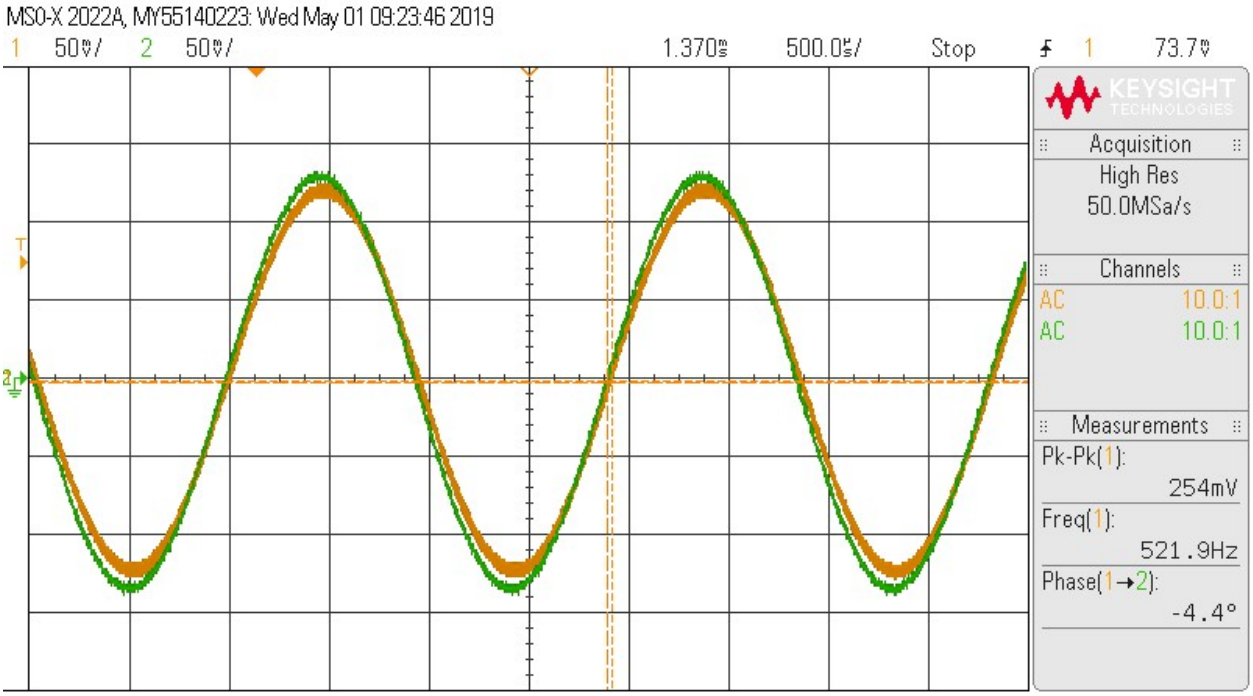

Figure 43: Two-Channel Variable Phase Sum Outputs at 0˚ Separation

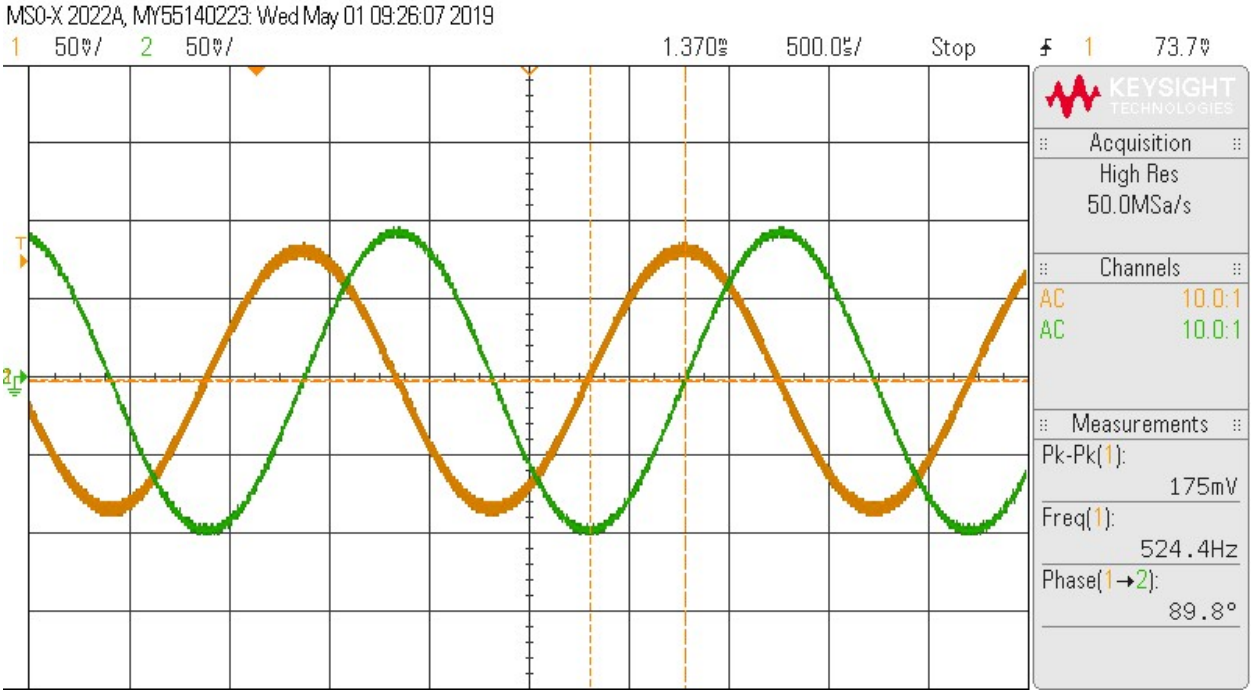

Figure 44: Two-Channel Variable Phase Sum Outputs at 90˚ Separation

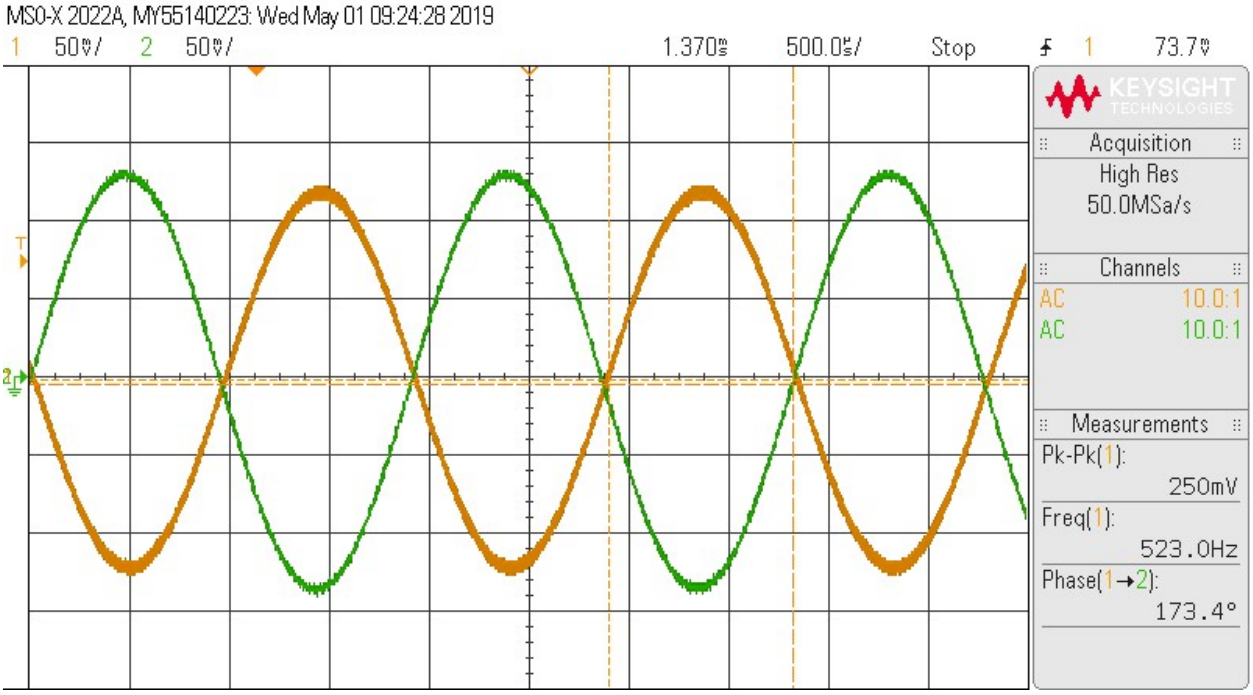

Figure 45: Two-Channel Variable Phase Sum Outputs at 180˚ Separation

Frequency Response

The plots of ***Figures 46-48*** experimentally measure the total frequency response of the frequency-manipulating portion of the overall system. Further, they justify the simulation-backed claims made in the **Design Refinements** section of a total passband magnitude variation of less than 1 dB after the addition of the Amplitude Inverse Filter. ***Figure 47*** is simply a zoomed in copy of ***Figure 46***.

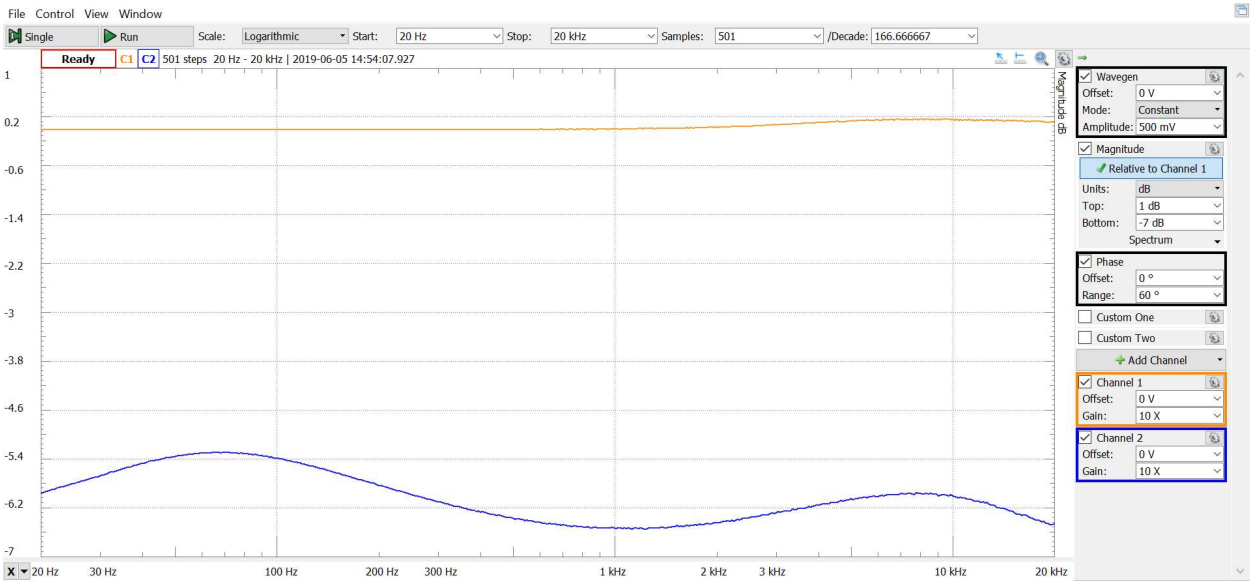

Figure 46: Normalized Experimental Magnitude Response of the System after the PPF Buffer

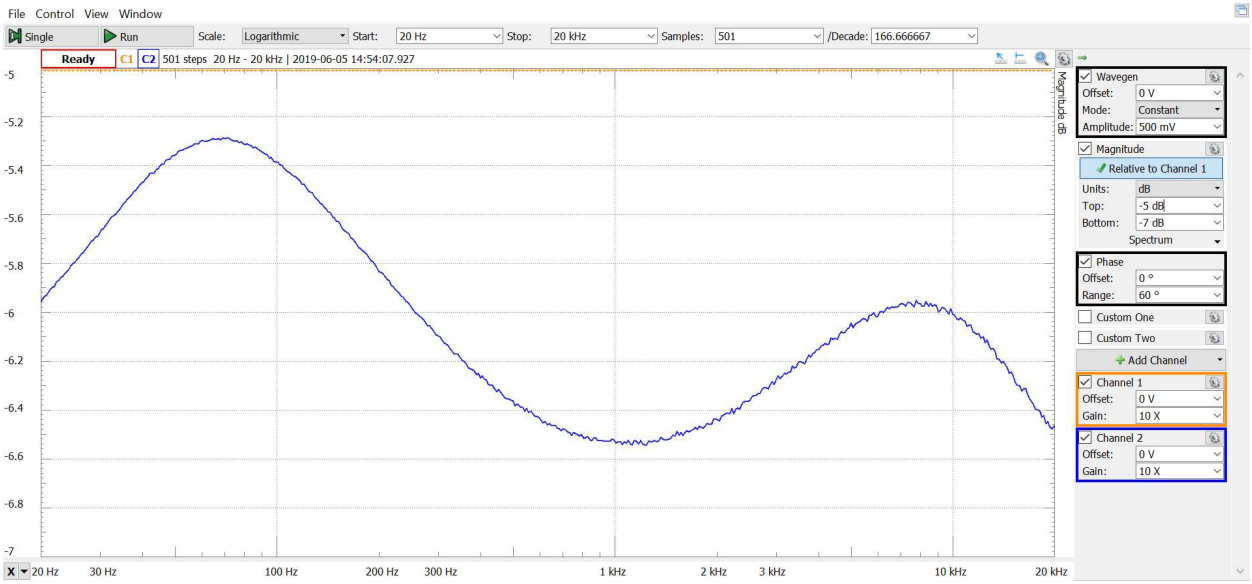

Figure 47: Normalized Experimental Magnitude Response of the System after the PPF Buffer

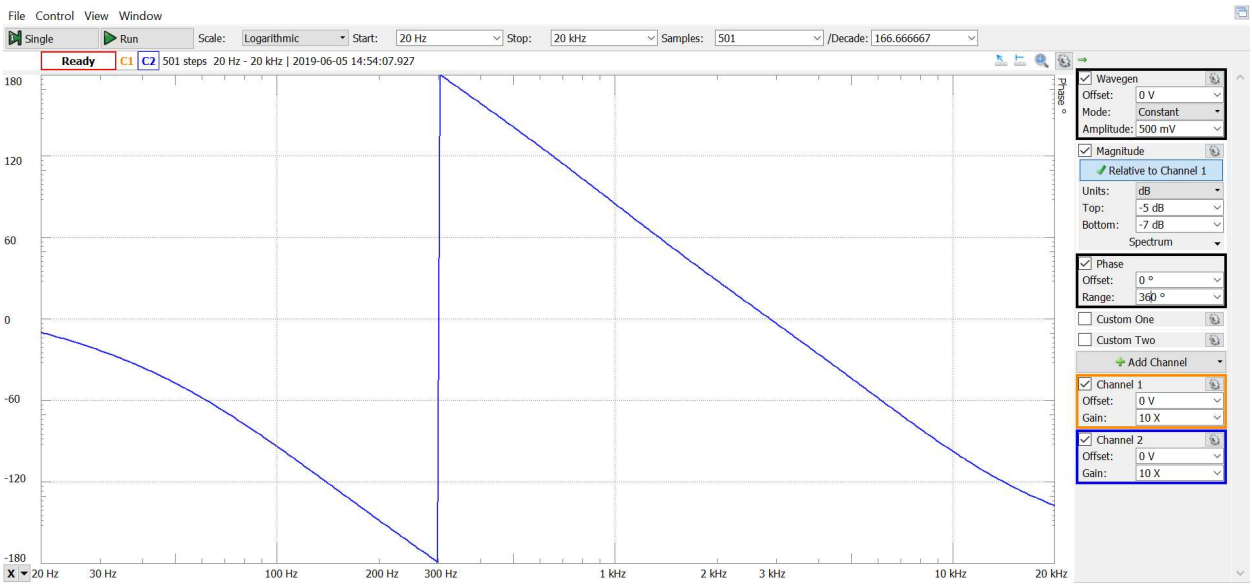

Figure 48: Normalized Experimental Phase Response of the System after the PPF Buffer

Miscellaneous

Phone Audio

To characterize the typical voltage output range of a consumer device, ***Figures 49-54*** contain oscilloscope captures of the output voltage of a Samsung Galaxy SVII cellphone while playing the same song at various volume levels from 1/15 to 15/15. Channel 1 corresponds to the Left output while Channel 2 corresponds to the Right output. The results of this test informed the design of the Stereo Audio Power Amplifier as described above.

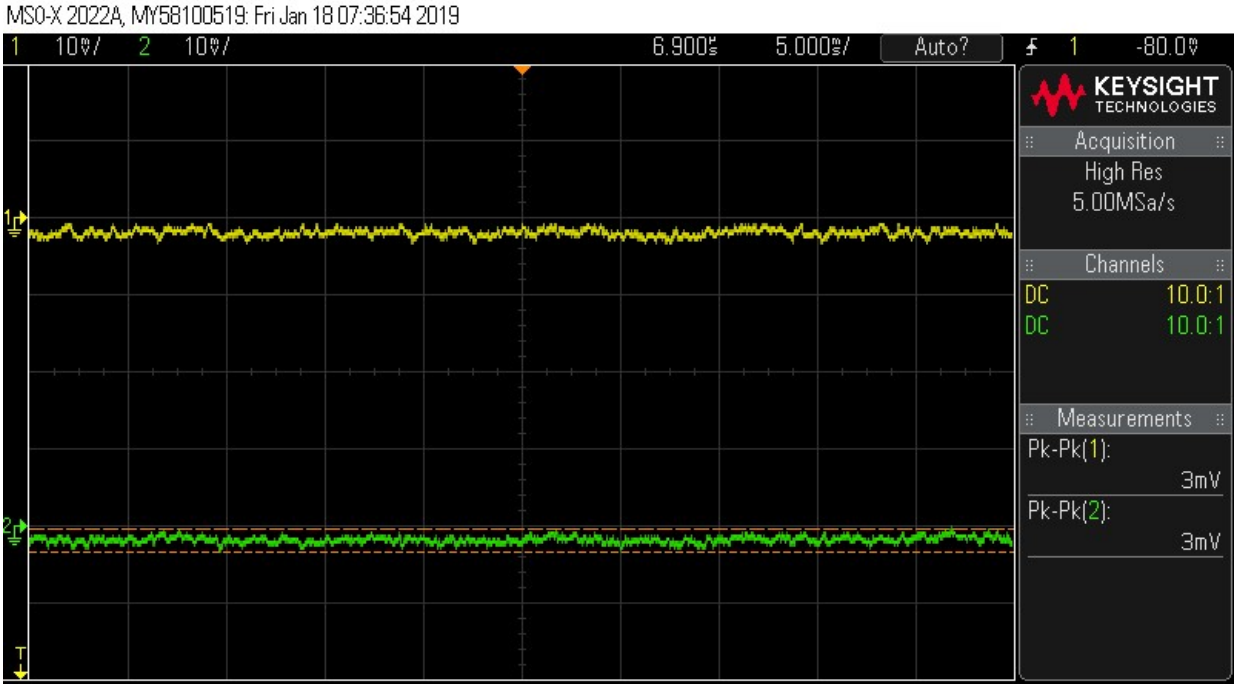

Figure 49: Phone Audio Level at Volume 1/15

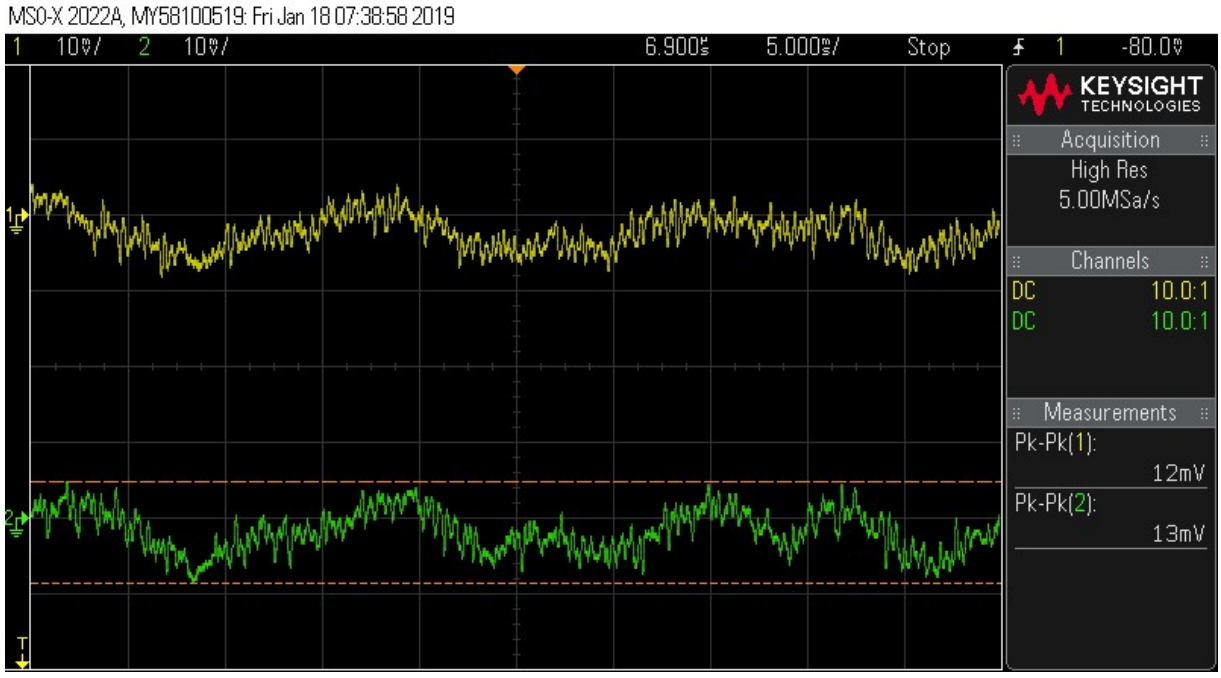

Figure 50: Phone Audio Level at Volume 5/15

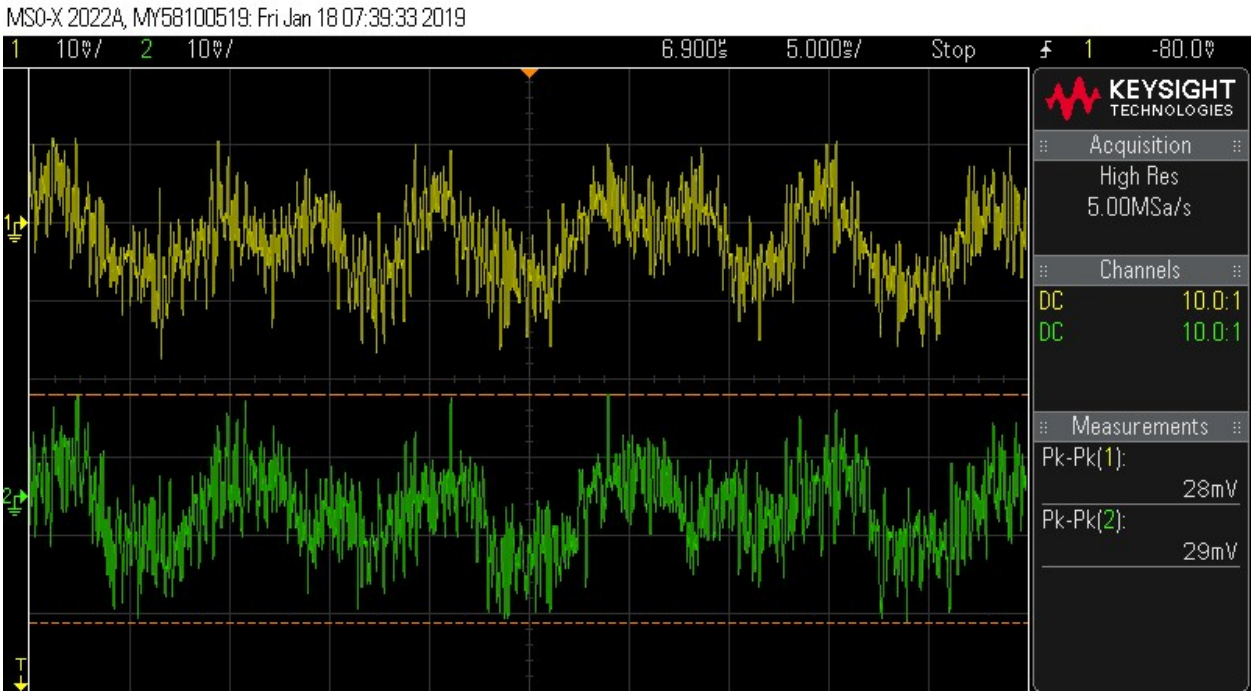

Figure 51: Phone Audio Level at Volume 7/15

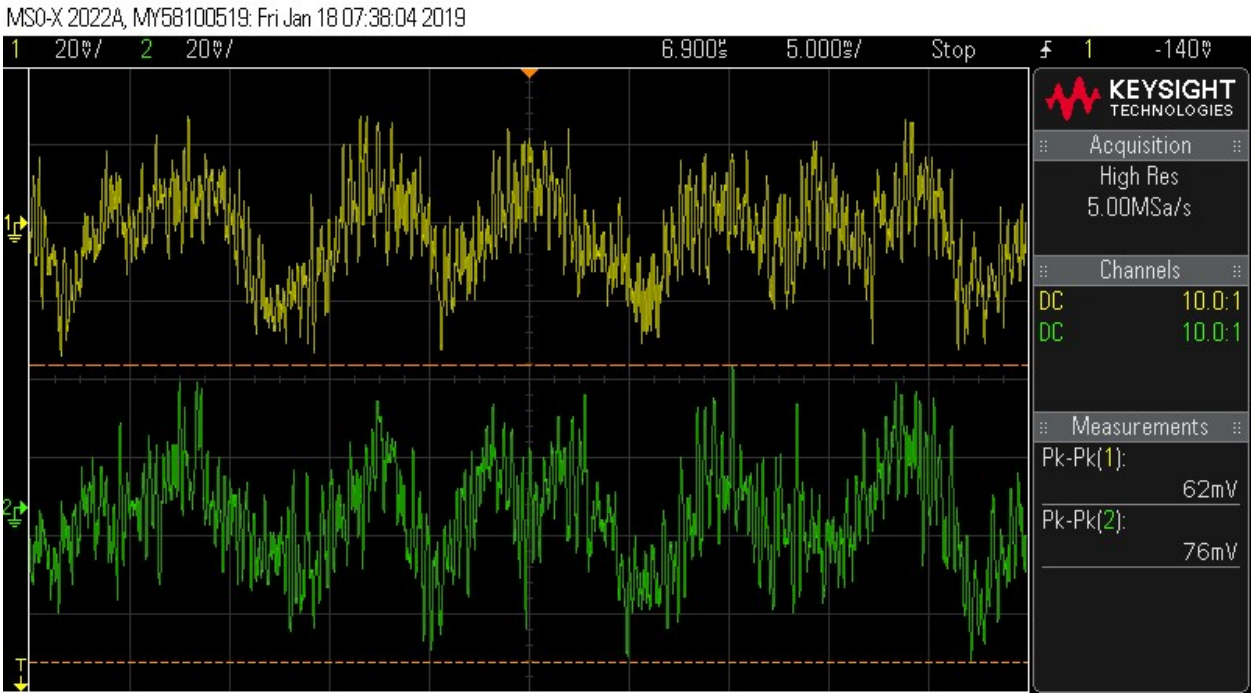

Figure 52: Phone Audio Level at Volume 9/15

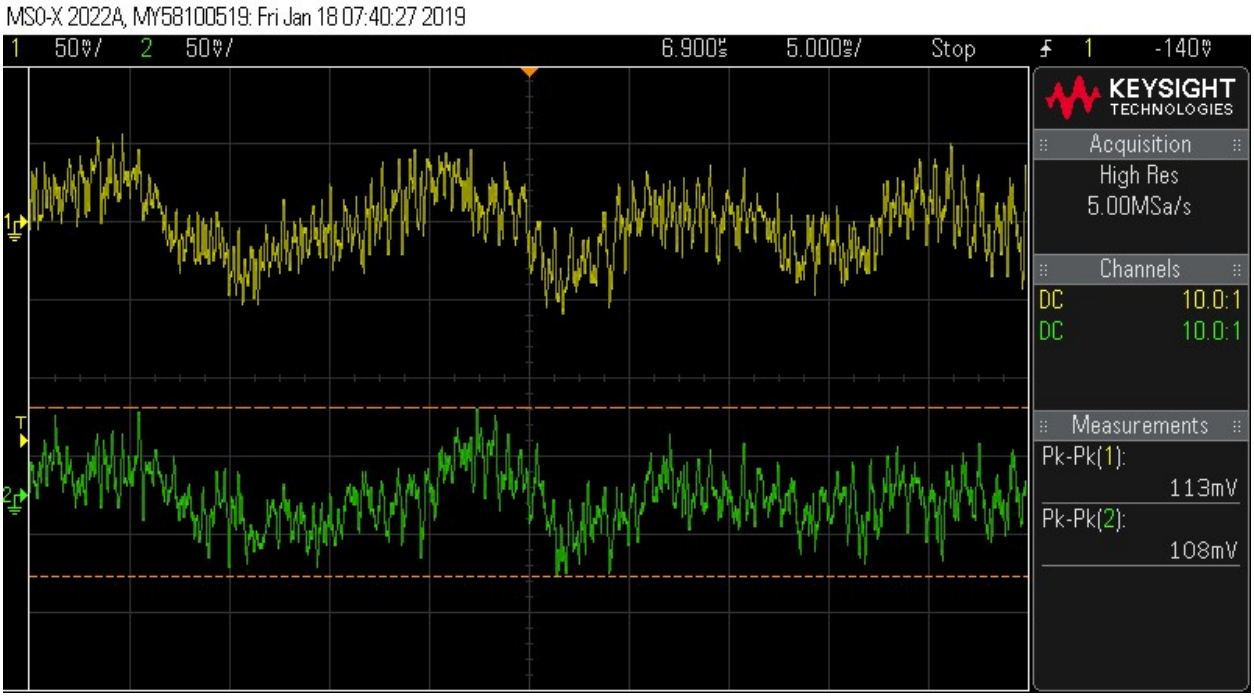

Figure 53: Phone Audio Level at Volume 10/15

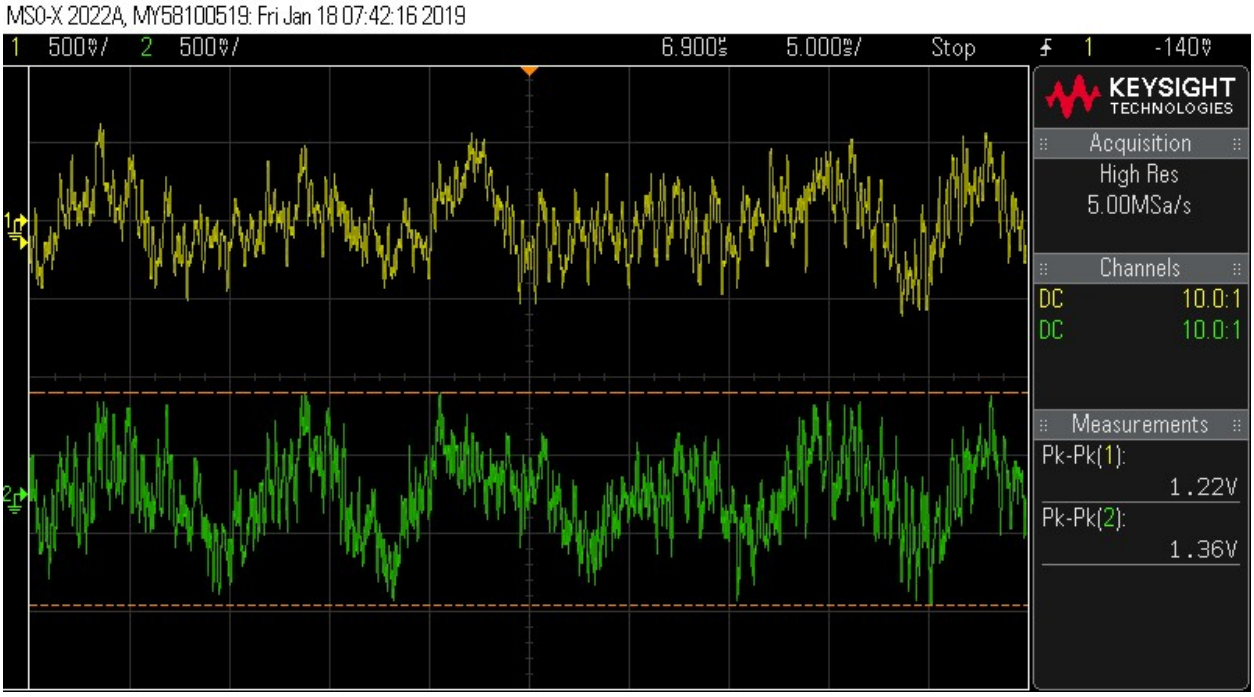

Figure 54: Phone Audio Level at Volume 15/15

Assembly

Easily visible in ***Figure 55*** below, each protoboard contains a single subsystem. Full system assembly consisted of aligning the subsystem boards, applying hot glue to the edges to ensure mechanical stability, and hardwiring most of the interconnects to ensure electrical stability.

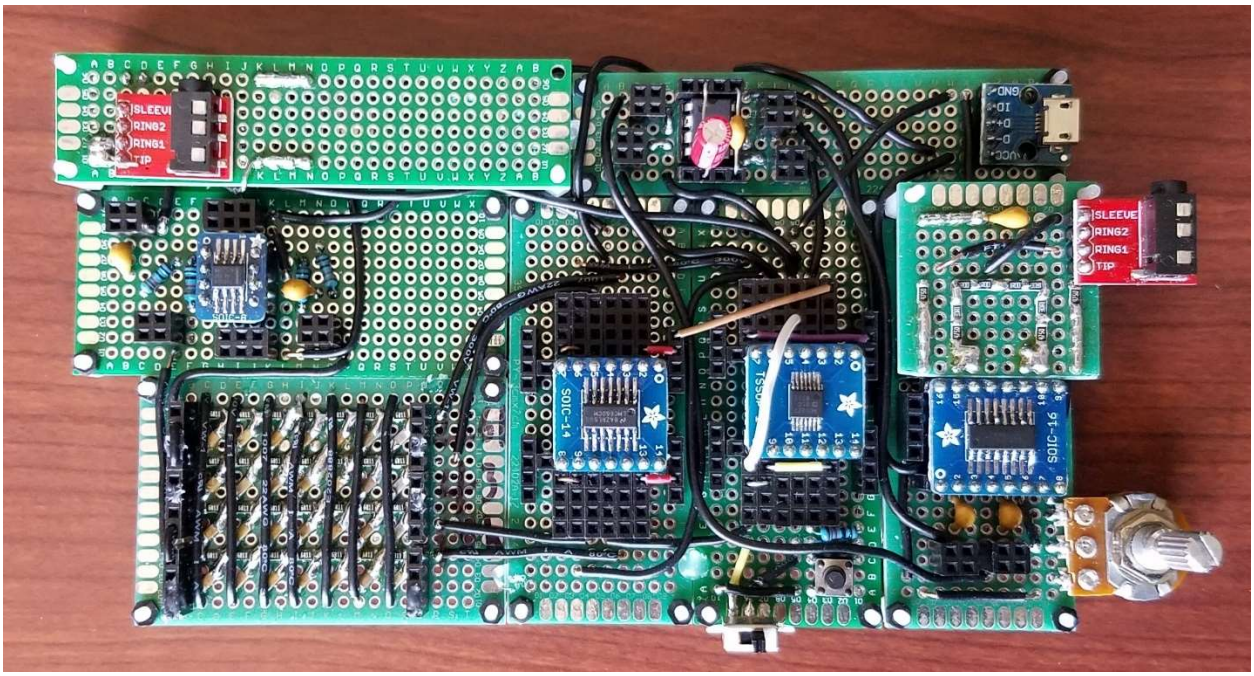

Figure 55: Final Assembled System Picture

Outstanding Issues & Possible Solutions

Due to both time constraints and the overall complexity of the system, there remains some issues not addressed by the design refinements described above. This section seeks to describe the current comprehension of the causes of these issues to assist future work as well as propose possible solutions.

6dB (1/2 Amplitude) Attenuation

As described above, a differential amplifier configured as a unity gain single to differential ended signaling converter provided well matched non-inverted and inverted copies of the input signal to the Polyphase Filter. However, this conversion inadvertently reduced the amplitude of each wave by half, as the distance between two parts of a differential signal constitutes the amplitude of the input. Since this reduced the gain by less than the 10 dB limit imposed by the specifications, and because of the warnings against increasing the closed loop gain under high capacitive loads in the component datasheet, this issue remained unaddressed in the final design. In future revisions, however, it would be a simple matter to design around this attenuation. One solution is to simply ensure that the differential amplifier chosen can handle the capacitive load of the Polyphase Filter while in a 2x gain configuration, while another is to add an inverting preamplifier with a gain of 2x, possibly utilizing spare op-amps on the chip used for the Amplitude Inverse Filter.

±0.5 dB Post-Polyphase Filter Magnitude Variance

Due to the mismatch between the flat top response of the Amplitude Inverse Filter and the parabolic behavior of the Polyphase Filter, even when well matched the overall system response exhibits a "wobble" in its frequency response of ±0.5 dB instead of the desired flat response. Though much improved over the massive mid-band drop present in the initial design, the response is not perfect. As such, future iterations of the design could utilize a higher order Amplitude Inverse Filter to allow more degrees of control in matching the response of the Polyphase Filter. For example, adding an unoptimized, iteratively tuned second stage composed of the same filter topology of the first stage with mildly changed component values alongside a slight re-tune of the first stage resulted in a dramatically improved simulated frequency response with less than 0.15 dB of total variation across the passband (See ***Figure 56***). As the current design only used one op-amp on a dual package chip, the change to a 4th order filter would not require any additional chips. For reference, the component values of the example filter consisted of R1 = 100 kΩ, C1 = 55 nF, R2 = 50 kΩ, C2 = 120 pF, R3 = 100 kΩ, C3 = 10 nF, R4 = 20 kΩ, C4 = 1.5 nF.

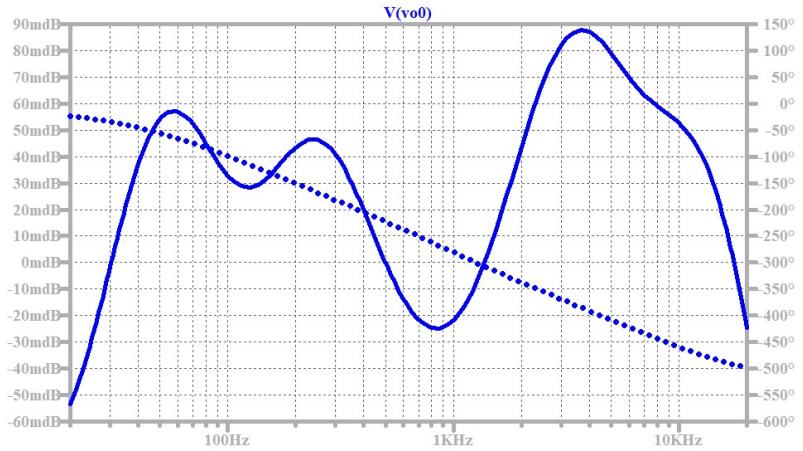

Figure 56: 4th Order Amplitude Inverse Filter & Polyphase Filter System Frequency Response

Crosstalk versus Output Attenuation Trade-off

As described in the **Design Refinements** section, adapting the differential outputs of the Class D amplifier to the single-ended output connector introduces a level of inefficiency and error. Though in the ideal case the differential-single ended COM-averaging network added would exhibit no crosstalk, this requires exact matching of the negative branch resistors to the total positive branch resistance which includes the resistive component of the load. Though precise 4-wire measurement of the total branch resistances avoids mismatch from component tolerances, the exact value of the load is not guaranteed, with variations of ±1 Ω seen in the 32 Ω headphones used. While the crosstalk present in the final design was not quantitatively measured, qualitative two-tone listening tests confirmed that a slight amount of audible crosstalk still existed at both the branch resistance of 507 Ω used and at resistances above 1 kΩ. However, increasing the branch resistance beyond 1 kΩ also resulted in a reduction of the max output volume to levels below the desired max output volume, as the amplifier used provides a maximum of +20 dB of amplification. This reduction in max output volume made it impossible to find a usable branch resistance at which crosstalk was inaudible. As such, one solution involves using a Class D amplifier with a higher max amplification to increase the max feasible branch resistance, while another necessitates matching smaller branch resistances to a difference of less than 1 Ω.

Polyphase Filter Phase Difference Accuracy versus Bandwidth Tradeoff

While the final design settled for a seven stage, 2.611 Notch-to-Notch ratio filter as the performance of ±3˚ of phase difference variation from ~43 Hz to 18.2 kHz met the specifications with the lowest stage count, improving both the bandwidth and phase accuracy is possible by using a filter with more stages and a lower Notch-to-Notch ratio. For example, the example designs included at the end of **Appendix B** include component values for a 13 stage, 1.771 Notch-to-Notch ratio filter which achieved an accuracy of ±0.4˚ across the entire standard audio band of 20 Hz to 20 kHz in simulation.

Incremental Phase Sum Control Accuracy and State Tracking

Since the final design utilized push-button control without any debounce mechanism, the actual control accuracy was much worse than the maximum accuracy of 1.41˚/step available from the 128-position digital potentiometer. Further, this simple control method lacked any way to track the exact position of the potentiometer and thus the phase difference between channels. While purely hardware means such as a one shot and counter could solve both issues, adding a microcontroller to the control path to allow for software debounce and state tracking presents itself as a much simpler option. As an added benefit, the availability of serial communication protocols such as SPI and I^2C on microcontrollers widens the range of usable digital potentiometers.

Power System

Neglected in both the initial design and refinement stages, a clean power source composes the final outstanding design issue. Assumed throughout most of the design and construction process was that the final design could directly obtain clean power from the 5V and GND lines of a micro-USB port connected to a common USB AC-DC wall converter, rendering a regulated power system unnecessary. Instead, this configuration produced audible, periodic variations related to the switching frequency of the AC-DC converter as seen in ***Figure 57*** and resulted in random drops in the rail voltage as seen in ***Figure 58***. While the periodic

variations are easily explained through interactions between the switching frequency of the AC-DC wall converter and the Class D switching frequency, the voltage drops likely stem from the 100 mA limit on current draw from an un-configured USB device as the pair of H-bridges that form the output stage of the Class D amplifier draw large amounts of instantaneous current. Due to encountering these issues very late in the assembly process, a generic 9V/5V external regulator board hardwired into a modified USB cable and a 9V battery powered the system. As this quick solution sacrifices efficiency and ease of use, including an actual power system could easily fix the problems encountered with true USB power. At a basic level, a system consisting of a USB configuration chip to increase the current limit to 500mA and a 5V LDO regulator to insulate the voltage rail against switching noise address the current issues. However, the further inclusion of rail isolation between the digital circuitry such as the Class D amplifier and digital potentiometer controls could minimize switching noise experienced by the analog circuitry. Building upon this further, the power system could also include USB communication capabilities, allowing more advanced software control over the various digital inputs of the Class D amplifier and digital potentiometer currently controlled through buttons and dials.

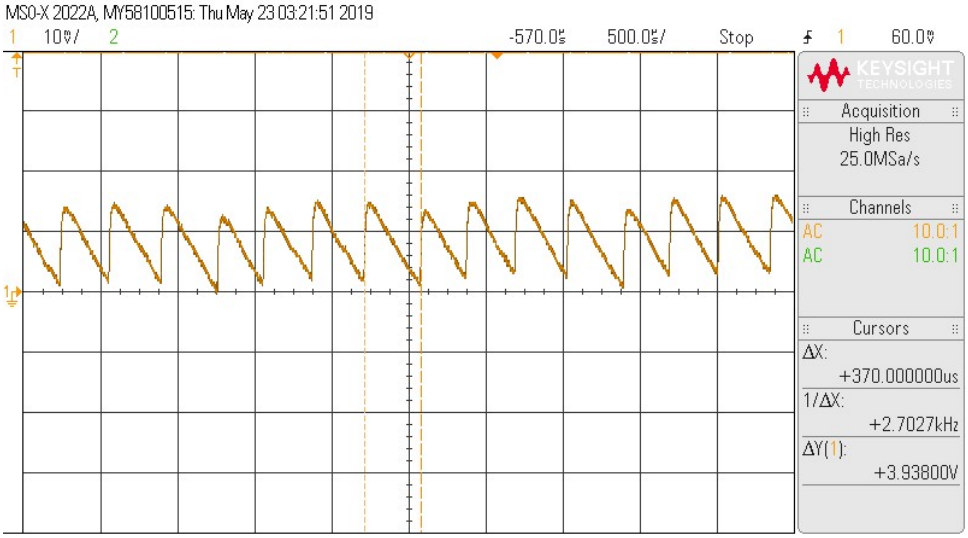

Figure 57: Voltage Supply Rail Audible Switching Noise

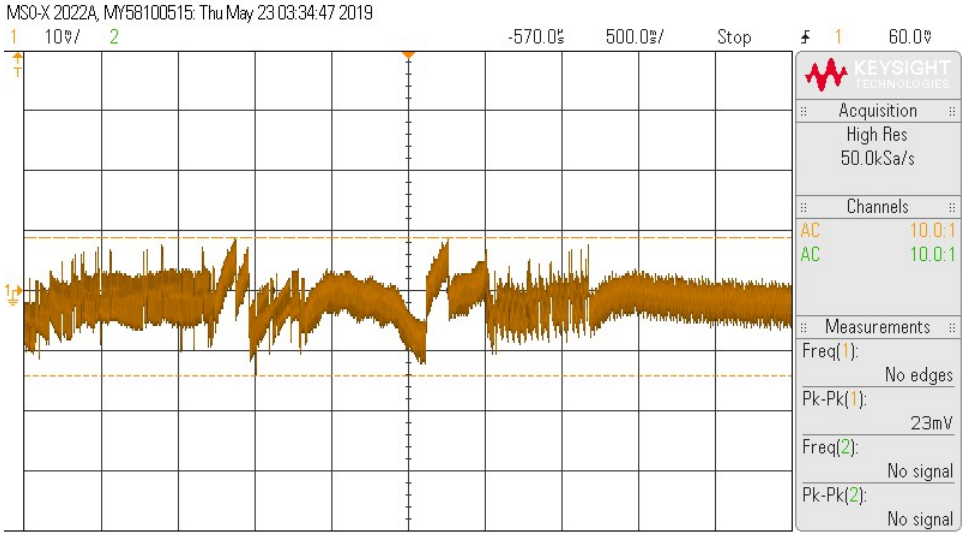

Figure 58: Voltage Supply Rail Non-Periodic Irregularities

Conclusions

Overall, the Pseudo-Stereo Audio Processor met its main goal: to produce a spatial auditory effect due to a fixed phase shift across the audible frequency range. As evidenced by both the data gathered above and qualitative listening tests performed, it outputs music largely uncorrupted by either distortion or noise, while accurately adding the Pseudo-Stereo effect on top. Despite slight issues with the micro-USB power source, it also largely met its secondary goal of being operable by someone no more familiar with electronics than the average person. Both volume and phase shift are controllable through dial and push-button interfaces, and both audio in and audio out have easy to use 3.5mm connectors, satisfying most of the control interface goals.

Unlike previous, quarter long analog electronics projects, many issues encountered such as inadequate buffering, inadequate supply bypassing, or arbitrarily broken ICs were largely avoided over the course of this project. Though the last stages of the project exposed a few design errors, they were largely fixable or inconsequential. As such, the most important experience obtained over the course of the project was the benefits of thorough planning. One of the main reasons this project went smoothly was because of the focus on research, discussion, and simulation before attempting to build a possibly broken circuit. Avoiding minor design mistakes through planning before they became issues streamlined the design process and allowed adequate time to remedy the few problems which did arise. Above all, building a device capable of producing a unique auditory effect is special on its own, as bringing electrical behavior out of test equipment and into human senses gives it life.

Appendix A: Senior Project Analysis

Project Title: Pseudo-Stereo Audio Processor
Student's Name: Zachariah Bunce **Student's Signature:**
Advisor's Name: Dr. Vladimir Prodanov **Advisor's Initials:** **Date:**

1. Summary of Functional Requirements

The audio processor introduces a quadrature phase shift onto a single-channel audio signal, producing multiple phase shifted versions of the input signal. It then outputs a combination of these phase shifted signals on a consumer audio connector, emulating a stereo-like auditory effect when connected to an external 2-channel capable audio system. This allows for easy post-production enhancing of the sound quality of a single-channel audio signal.

2. Primary Constraints

Due to the high sensitivity of normal human hearing to certain types of signal distortion [4], the low-cost requirement forms the primary limitation on the project. As accurate systems create both a large amount of upfront development cost and increase long-term production costs, balancing accuracy and cost proved difficult. See Chapter 2 for more in-depth description of the constraints placed on the project based on the marketing requirements and technical specifications.

3. Economic

The project impacts all four forms of capital. For Human Capital, it increases the quality of small-scale recording artists, allowing them to produce spatial qualities in recorded music previously lacking spatial effects. The project also provides a method for small-scale recording studios to increase productivity, resulting in larger revenues at lower costs and increasing Financial Capital. Further, these two impacts combine to form Manufactured Capital, as the project acts as a tool to enable the higher productivity and quality impacts mentioned previously. However, the project negatively impacts Natural Capital due to its use of limited natural materials required by electrical components.

The initial design process contains most of the project costs due to the high-cost design labor and expensive test equipment necessary to ensure a complete and robust product. The rest result from minimal long-term production. In contrast, the benefits accrue over the entire lifespan of the product resulting from the project due to the benefits occurring through general use of the product. Specifically, the expected design time, production labor, verification equipment, and various material components result in a total project cost of $10231. The expected funding sources consist of a combination of the designer paying for their own time and prototyping components, and Cal Poly through the availability of test equipment for use by the designer.

Table 6: Initial Material Cost Estimate

Type	Quantity	Design Cycles	Cost/Unit ($)	Cost ($)
Resistors (1% Tol.)	44	8	0.03	10.56
Capacitors (10% Tol.)	44	8	0.1	35.2
ICs	5	8	2	80
Connectors	8	8	0.5	32
PCB	1	8	5	40
Total Cost per Design				24.72
Total Material Cost				**197.76**

Table 7: Initial Equipment Cost Estimate

Type	Quantity	Cost/Unit ($)	Cost ($)
Oscilloscope	1	400	400
Power Supply	1	300	300
Multimeter	2	10	20
Function Generator	1	250	250
Oscilloscope Probes	2	7	14
Misc. Connection Wires	10	3	30
2-Channel Earbuds	2	10	20
Total Equipment Cost			**1034**

Based on the costs outlined in ***Table 6*** and ***Table 7,*** and using the process described in Section 4, the designer expects a gross yearly profit of $528 for themselves.

As seen in ***Figure 59*** and ***Figure 60*** below, expected completion of the design process occurs around June 2019. Production and sale of the audio processor begins upon completion of this project. Allowing for 3 months of manufacturing and delivery time after project completion, the final product would release by September 2019. Once available, the expected lifespan ranges from 5 to 10 years based on the speed at which currently common audio and power connectors become obsolete. Due to the simple nature and largely passive component implementations of the many options found for the necessary sub systems ([5], [6], [7]), normal electrical usage should not further limit the lifespan. This expectation also leads to negligible maintenance costs. Furthermore, the low power design keeps operation costs to a minimum, as power consumed contains most of these costs.

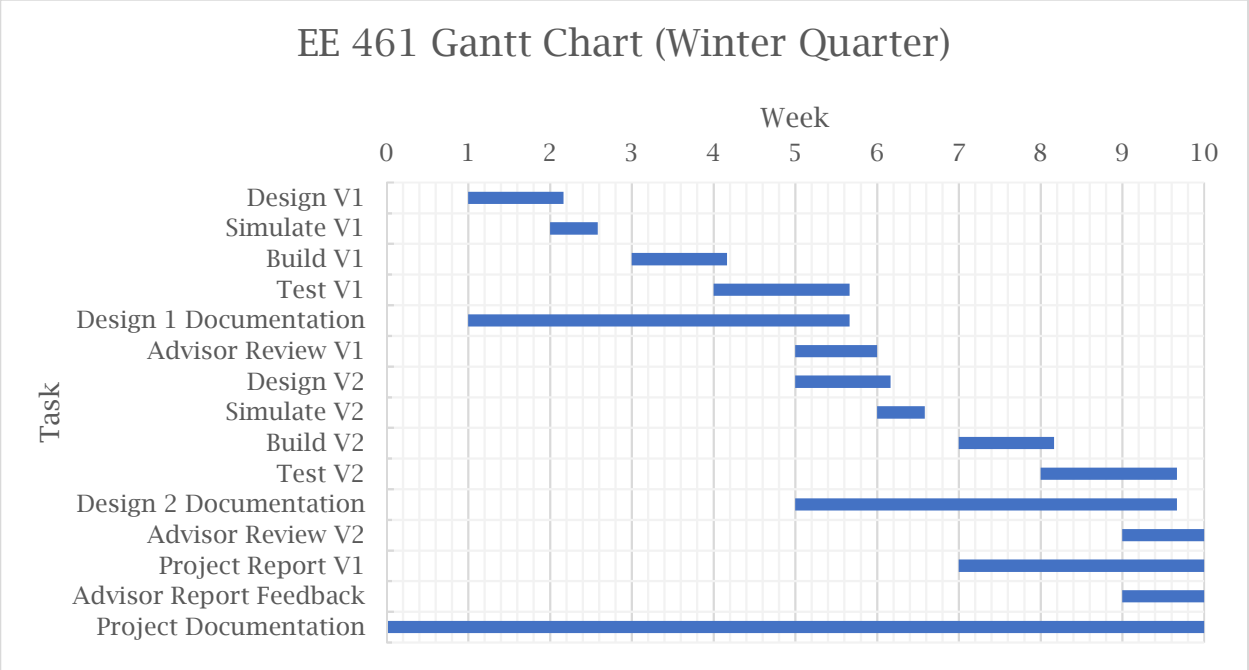

Figure 59: Winter Quarter 2019 Initial Estimated Development Time

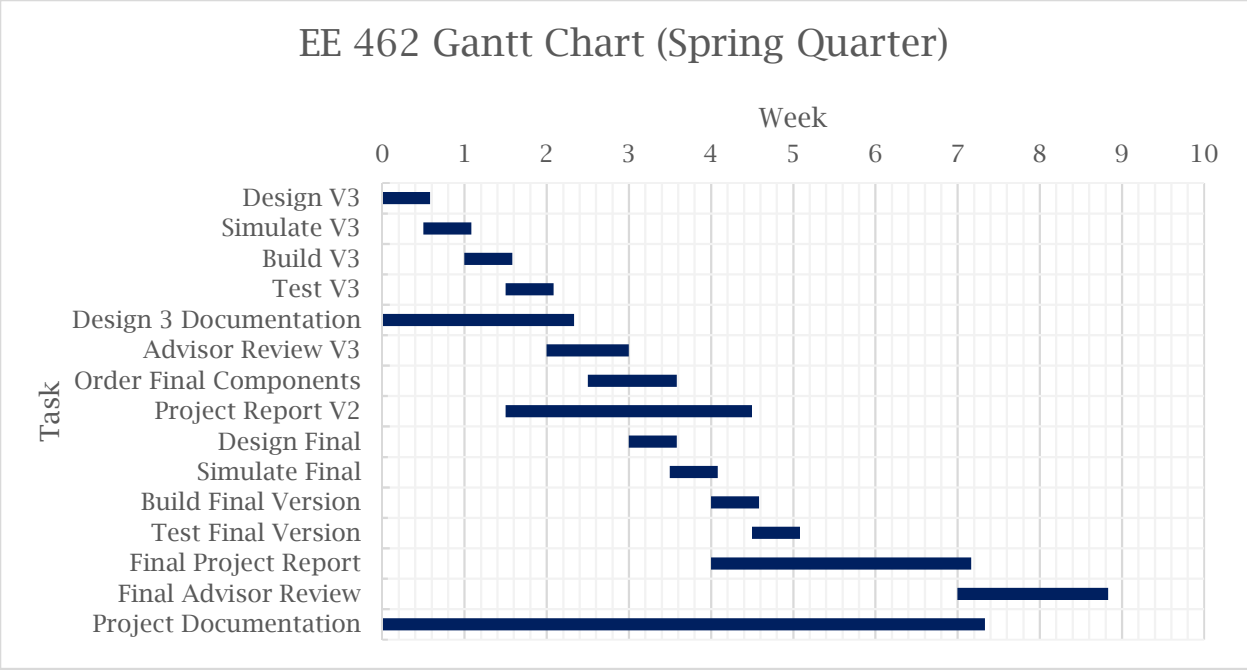

Figure 60: Spring Quarter 2019 Initial Estimated Development Time

4. If manufactured on a commercial basis:
Estimating a sale of 100 devices per year as a niche commercial product, a purchase price of $30 allows for a total yearly revenue of $3000 from sales of the audio processor. This revenue and the estimated manufacturing cost of $24.72 per device results in an expected gross profit of $528 per year. Combining this profit estimate with the total cost estimate from ***Table 3*** *of* $10231.60, it would take 20 years to recoup the initial cost. The low-power specification of an average power use less than 0.5 W and the average electricity price in California of $0.155 per kWh results in an estimated user operation cost of $6.79 per year.

5. Environmental
Though the use of the audio processor does not directly affect any environments, as it simply performs electrical operations on audio signals, it consumes electrical power, whose generation indirectly affects a variety of environments depending on the origin of the power consumed. Hydroelectric power, for example, greatly affects fish populations, river ecosystems, and land use due to the large dams necessary to produce it.

The manufacturing process also has many environmental effects, mainly concerning the origin of materials inside electrical components and the disposal of chemicals from the manufacture. The disposal methods of these chemicals may adversely affect the ecosystems near disposal sites without proper precautions, resulting in harm or destruction to species reliant on damaged facets of the ecosystem. The mining and purification processes to extract and prepare the necessary raw materials may further harm the same and other ecosystems through waste disposal and heavy machinery use.

6. Manufacturability
Due to the relative ease in manufacturing modern printed circuit boards and enclosures for a hand-held size device, simply ensuring that plans account for the significant amount of time that PCB fabrication takes encompasses the main challenge in manufacturing. Furthermore, the widespread availability of automatic pick-and-place machines in commercial manufacturing avoids potential assembly issues relating to the attachment of small I/O pads and compact chip footprints to the small PCB necessary for meeting the spatial specifications defined in **Requirements & Specifications**

7. Sustainability
As the project design focuses on ease of use and robustness, minimal maintenance issues are expected. However, the rare materials used in the manufacture of electrical components causes the project to negatively impact sustainable resource use, as any contribution only further increases the unstainable current usage. With a longer design timeline, performance optimizations could reduce the total design size while maintaining required accuracy, decreasing the projects contribution to the unsustainable use of resources. However, upgrading the design would also result in more design iterations, resulting in a larger initial material use.

8. Ethical
The environmental effects of the electronics manufacturing processes required by the project pose an ethical dilemma. Though often buying electrical components manufactured in certain foreign countries decreases the cost, these components may come from manufacturing plants with less environmental restrictions and regulatory oversight than those manufactured in countries with strong and proven environmental protections. This leads to the possibility that reducing material costs through certain component imports creates a greater hidden environmental impact of the project. Expanding on that choice creates two options, to either source expensive components from manufacturers in countries with strong environmental protections or to source cheap components from manufacturers in countries with weak environmental protections. Utilizing the ethical framework of Utilitarianism, sourcing components from manufacturers subject to strong environmental protections forms the ethical choice. As Utilitarianism calls for the greatest good for the greatest number, the benefits produced through decreasing the production costs of one product does not outweigh the harm caused to generations of people near the manufacturing plant now living in an unsafe environment partially created by the manufacturing process, as harmful environmental effects often persist long after creation. As such, components the design uses must come from locations with strong environmental protections, and any fabrication must occur under manufacturers who ensure the environment is not negatively impacted by their processes to maintain the ethical standard imposed by Utilitarianism.

Furthermore, the IEEE Code of Ethics agrees with the result previously obtained. As stated in the first tenet, decisions made must stay consistent with the safety, health, and welfare of the public. Choosing to possibly harm the environment runs counter to preserving the health of the public living within the nearby environment. Thus, the choosing of manufacturers, component distributors, and assembly locations must occur under careful consideration to avoid any conflicts with this ethical code.

Expanding upon this argument, the IEEE Code of Ethics provides a positive framework beyond merely avoiding unethical choices. By expanding the use of polyphase filters beyond mere communications applications found in [2], [3], [5], [6], and [7], this project provides a widening of the technology available to audio processors. Improving upon the current technological understanding of polyphase filters, the Pseudo-Stereo Audio Processor fulfills the fifth tenet of the IEEE Code of Ethics and avoids repeating applications. Furthermore, the design choices made promoting ease of use and simplicity provide another positive ethical benefit under the tenth tenet of the IEEE Code of Ethics by ensuring the possibility of use of the product by a wide variety of customers, assisting their professional development regardless of experience with electrical filters.

9. Health and Safety

Due to the USB powered marketing requirement, there exists little electrical danger during use. However, PCB manufacture requires many corrosive and caustic chemicals, leading to possible safety concerns into the proper use, transport, and disposal procedures of these chemicals to prevent injury during manufacture.

10. Social and Political

The combination of tariff uncertainties and the current political administrations economic antagonism of certain trading partners, specifically China, means the manufacturing process may fall victim to increased costs, as Chinese manufacturers create many necessary electrical components.

Overall, the project directly benefits small-scale and future expansions of recording studios by providing a low-cost alternative in producing stereo audio. This both directly and indirectly affects these stakeholders, as it directly provides cost savings over equivalent products, decreasing overhead, and indirectly makes the music produced more valuable by enhancing the sound quality with a spatial component. Conversely, the project negatively impacts producers of current stereo audio solutions by displacing the current market share of their products. This comprises a direct impact on these stakeholders, as the project openly competes against their interests. However, the project also indirectly benefits these same stakeholders as the filter methodologies the project applies may eventually supplement traditional methods of achieving stereo audio, enhancing their solutions rather than just competing with them.

11. Development

A new technique used during the design process consisted of Monte Carlo analysis to determine if a design met specifications across the full component value tolerance and temperature ranges. Additionally, [2], [3], [5], [6], and [7] provided many possible variations on passive and active polyphase filter topologies, illuminating the different options available to provide the core all-pass functionality the design requires.

Appendix B: Polyphase Filter Design Spreadsheet

In comma-delineated text format (.csv)

```
This spreadsheet calculates R&C of a 5-stage poly-phase filter; 'critical' freq. equidistant on a log
scale.,,,,,,,,,,,,,,,,,,,,,,,,,,,,
The table explores 3 possible cases realizing desired time-constants.,,,,,,,,,,,,,,,,,,,,,,,,,,,,
,,,,,,,,,,,,,,,,,,,,,,,,,,,,
Higest 'Notch' Freq.,9954,Hz,Variable,,,,,,,,,,,,,,,,,,,,,,,,
Lowest 'Notch' Freq.,462,Hz,Variable,,,,,,,,,,,,,,,,,,,,,,,,
Number of Sections,5,,Variable,,"For wider bandwidths, more stages are needed to maintain constant phase shift
across the passband",,,,,,,,,,,,,,,,,,,,,,
Notch-to-Notch Ratio,2.154,2.154,Calculated,,,,,,,,,,,,,,,,,,,,,,,,
Per Phase Resistance (Fixed R),0.5235,kOhm,Variable,,Vary to keep capacitances in usable
range,,,,,,,,,,,,,,,,,,,,,,
Total Resistance (per phase),3.6645,kOhm,Calculated,,,,,,,,,,,,,,,,,,,,,,
,,,,,,,,,,,,,,,,,,,,,,,,,,,,
,Three Expreme Cases of R and C scaling (at a fixed R_tot),,,,,,,,,,,,,,,,,,,,,,,,,,,,
,Case 1: Fixed R,,Case 2: Fixed C,,Case 3: R & C change,,,,,,,,,,,,,,,,,,,,,,
"f_notch, Hz","R, KOhm","C, nF","C, nF","R, kOhm","R, kOhm","C, nF",,,,,,,,,,,,,,,,,,,,,,
462,0.7329,470.04,171.7,2.01,1.37,251.67,,,,,,,,,,,,,,,,,,,,,
995,0.7329,218.170,171.7,0.93,0.93,171.46,,,,,,,,,,,,,,,,,,,,,
2144,0.7329,101.264,171.7,0.43,0.64,116.81,,,,,,,,,,,,,,,,,,,,,
4620,0.7329,47.0020,171.7,0.20,0.43,79.58,,,,,,,,,,,,,,,,,,,,,
9954,0.7329,21.81613,171.7,0.09,0.29,54.22,,,,,,,,,,,,,,,,,,,,,
21446,0.7329,10.126,171.7,0.04,24.97,0.30,,,,,,,,,,,,,,,,,,,,,
46204,0.7329,4.700,171.7,0.02,17.01,0.20,,,,,,,,,,,,,,,,,,,,,
99544,0.7329,2.1815,171.7,0.01,11.59,0.14,,,,,,,,,,,,,,,,,,,,,
214463,0.7329,1.013,171.7,0.00,7.90,0.09,,,,,,,,,,,,,,,,,,,,,
462053,0.7329,0.4700,171.7,0.00,5.38,0.06,,,,,,,,,,,,,,,,,,,,,
995477,0.7329,0.218,171.7,0.00,5.38,0.03,,,,,,,,,,,,,,,,,,,,,
2144717,0.7329,0.101,171.7,0.00,#REF!,#REF!,,,,,,,,,,,,,,,,,,,,,
4620713,0.7329,0.047,171.7,0.00,#REF!,#REF!,,,,,,,,,,,,,,,,,,,,,
Total kOhm & nF (per phase),3.6645,858.3,858.3,4,3.6645,673.74,,,,,,,,,,,,,,,,,,,,,
,,,,,,,,,,,,,,,,,,,,,,,,,,,,
2.154NtN,3 vals,~1 Decade All-Pass for 5S w/ +-1deg variation,,,,,1 per 4,,~2 Decade All-Pass for 7S w/ +-1deg
variation,,,,,,9S achieves +-1.5deg from 30Hz-18kHz (2.154NtN),,,,,,,,,,,,,
2.612NtN,5 val,~1.5 Decade All-Pass for 5S w/ +-3deg variation,,,,,1 per 5,,~2.5 Decade All-Pass for 7S w/ +-
3deg variation,,,,,,13S achieves +-0.4deg from 20Hz-20kHz (1.8NtN),,,,,,,,,,,,,
3.152NtN,2 vals,~2 Decade All-Pass for 5S w/ +-5deg variation,,,,,1 per 6,,~3 Decade All-Pass for 7S w/ +-5deg
variation,,,,,,,,,,,,,,,,,,,,
,,,,,,,,,,,,,,,,,,,,,,,,,,,,
3.153 NtN,N1 Var,N2 Var,N3 Var,N4 Var,N5 Var,Sum,flow,fhigh,,,,,,,,,,,,,,,,,,,,
2.260kO,0.039,68.170,54.264,32.0020,17.11613,171.591,107,10573,Notch BW,,,,,,,,,,,,,,,,,,
2.26k,470,150,47,15,4.7,1.354,124,18k,Pass BW,+-5deg,,,,,,,,,,,,,,,,,,
,,,,,,,,,,,,,,,,,,,,,,,,,,,,
2.612 NtN,N1 Var,N2 Var,N3 Var,N4 Var,N5 Var,Sum,flow,fhigh,,,,,,,,,,,,,,,,,,,,
1.089kO,0.039,38.170,33.264,20.0020,11.81613,103.291,222,10340,Notch BW,,,,,,,,,,,,,,,,,,
1.07k,470,180,68,27,10,1.855,272,17.3k,Pass BW,+-3deg,,,,,,,,,,,,,,,,,,
,,,,,,,,,,,,,,,,,,,,,,,,,,,,
2.155 NtN,N1 Var,N2 Var,N3 Var,N4 Var,N5 Var,Sum,flow,fhigh,,,,,,,,,,,,,,,,,,,,
0.4342kO,0.039,-1.830,1.264,0.0020,-0.18387,3.319,557,12002,Notch BW,,,,,,,,,,,,,,,,,,
0.432k,470,220,100,47,22,3.330,720,18.2k,Pass BW,+-1deg,,,,,,,,,,,,,,,,,,
,,,,,,,,,,,,,,,,,,,,,,,,,,,,
,,,,,,,,,,,,,,,,,,,,,,,,,,,,
3.152 NtN,N1 Var,N2 Var,N3 Var,N4 Var,N5 Var,N6 Var,N7 Var,Sum,flow,fhigh,,,,,,,,,,,,,,,,,,
9.538kO,0.039,68.170,54.264,32.0020,17.11613,8.62602,4.23002,184.447,35.5,34859,Notch BW,,,,,,,,,,,,,,,,
9.53k,470,150,47,15,4.7,1.5,0.47,1.314,29,18.1k,Pass BW,+-5deg (Final dip outside frange),,,,,,,,,,,,,,,,
,,,,,,,,,,,,,,,,,,,,,,,,,,,,
2.611 NtN,N1 Var,N2 Var,N3 Var,N4 Var,N5 Var,N6 Var,N7 Var,Sum,flow,fhigh,,,,,,,,,,,,,,,,,,
6.813kO,0.039,38.170,33.264,20.0020,11.81613,6.22602,3.20002,112.717,49.7,15757,Notch BW,,,,,,,,,,,,,,,,
6.81k,470,180,68,27,10,3.9,1.5,1.719,43,18.2k,Pass BW,+-3deg,,,,,,,,,,,,,,,,
,,,,,,,,,,,,,,,,,,,,,,,,,,,,
2.154 NtN,N1 Var,N2 Var,N3 Var,N4 Var,N5 Var,N6 Var,N7 Var,Sum,flow,fhigh,,,,,,,,,,,,,,,,,,
2.491kO,0.039,-1.830,1.264,0.0020,-0.18387,0.1260,0.00002,3.445,135.9,13598,Notch BW,,,,,,,,,,,,,,,,
2.43k,470,220,100,47,22,10,4.7,3.522,127,15.2k,Pass BW,+-1deg,,,,,,,,,,,,,,,,
,,,,,,,,,,,,,,,,,,,,,,,,,,,,
,,,,,,,,,,,,,,,,,,,,,,,,,,,,
1.771 NtN,N1 Var,N2 Var,N3 Var,N4 Var,N5 Var,N6 Var,N7 Var,N8 Var,N9 Var,N10 Var,N11 Var,N12 Var,N13
Var,Sum,flow,fhigh,,,,,,,,,,,,
16.9kO,0.039,-51.830,-48.736,-34.998,-25.184,-16.874,-10.300,-6.018,-3.687,-2.230,-1.282,-0.719,-
0.423,202.320,37.21,35359,Notch BW,,,,,,,,,,,,
16.9k,470,270,150,82,47,27,15,8.2,4.7,2.7,1.5,0.82,0.47,9.144,20,20k,Pass BW,+-0.4deg,,,,,,,,,
```

References

[1] S. Rosen and P. Howell, *Signals and Systems for Speech and Hearing*, 2nd ed. Bingley, UK: Emerald Group Publishing Limited, 2011, p. 163.

[2] S. Johnston, *Complex Filters as a Cascade of Buffered Gingell Structures: Design from Band-Stop Constraints*. M.S. [Thesis]. San Luis Obispo, CA: Cal Poly, 2016. [Online]. Available: DigitalCommons@CalPoly, https://digitalcommons.calpoly.edu/theses/1638/ [Accessed Oct. 16, 2018].

[3] N. Hay, *Complex Filters as Cascade of Buffered Gingell Structures: Design from Band-Pass Constraints*. M.S. [Thesis]. San Luis Obispo, CA: Cal Poly, 2017. [Online]. Available: DigitalCommons@CalPoly, https://digitalcommons.calpoly.edu/theses/1731/ [Accessed Oct. 19, 2018].

[4] F. Massa, "Permissible Amplitude Distortion of Speech in an Audio Reproducing System", *Proceedings of the Institute of Radio Engineers*, vol. 21, no. 5, pp. 682-689, May 1933. [Online]. Available: IEEE Xplore, https://ieeexplore.ieee.org/document/1685371 [Accessed Oct. 20, 2018].

[5] K. Schmidt, “Phase-Shift Network Analysis and Optimization”, *QEX*, Aug. 1994. [Online]. Available: http://fermi.la.asu.edu/w9cf/articles/phase/index.html [Accessed Oct. 20, 2018].

[6] W. J. Niessen, "Understanding and Designing Sequence Asymmetric Polyphase Networks”, *Antennoloog.nl*, Aug. 25, 2006. [Online]. Available: http://antennoloog.nl/data/documents/Understanding_and_designing_Polyphase_networks_V4.0.pdf [Accessed Oct. 20, 2018].

[7] M. J. Gingell, “Single Sideband Modulation using Sequence Asymmetric Polyphase Networks,” *Electrical Communications*, vol. 48, no. 1–2, pp. 21–25, 1973.

[8] W.M Hartmann, "Some psychoacoustical experiments with all-pass networks," *American Journal of Physics* 47, 29 (1979). [Online]. Available: Scitation, https://aapt.scitation.org/doi/abs/10.1119/1.11659 [Accessed Nov. 12, 2018].

[9] Andrés Cabrera, “Pseudo-stereo Techniques: Csound Implementations,” *CSOUND Journal* vol. 14 (Winter 2011). [Online]. Available: http://www.csounds.com/journal/issue14/PseudoStereo.html [Accessed Jun. 12, 2019]

[10] Charles Kitchin, “If All Else Fails, Read This Article. Avoid Common Problems When Designing Amplifier Circuits” *Analog Dialogue* vol. 41, (Aug. 2007). [Online]. Available: https://www.analog.com/en/analog-dialogue/articles/common-problems-when-designing-amplifier-circuits.html [Accessed Jun. 12, 2019]

[11] Texas Instruments, “Ultra Low-Power, Rail-to-Rail Output, Fully Differential Amplifier”. THS4531A datasheet. Dec. 2012 [Revised Jan. 2016]. Available: http://www.ti.com/lit/ds/symlink/ths4531a.pdf [Accessed Jun. 12, 2019]

[12] Diodes Incorporated, “3W Stereo Class-D with DC Volume, Power Limit and Anti-Saturation”. PAM8008 datasheet. Oct. 2012. Available: https://www.diodes.com/assets/Datasheets/PAM8008.pdf [Accessed Jun. 12, 2019]